Performance Targets for Electric Vehicle Batteries

by

Michael Tse-Gene Chang

B.S. Computational Engineering Science
University of California, Berkeley (2011)

Submitted to the Engineering Systems Division
in partial fulfillment of the requirements for the degree of

Master of Science in Technology and Policy

at the

MASSACHUSETTS INSTITUTE OF TECHNOLOGY

February 2015

Author .....
Technology and Policy Program
Engineering Systems Division
October 31, 2014

Certified by .....
Jessika E. Trancik
Atlantic Richfield Career Development Assistant Professor in Energy Studies
Thesis Supervisor

Accepted by .....
Dava J. Newman
Professor of Aeronautics and Astronautics and Engineering Systems
Director, Technology and Policy Program

Performance Targets for Electric Vehicle Batteries

by

Michael Tse-Gene Chang

Submitted to the Engineering Systems Division
on October 31, 2014, in partial fulfillment of the
requirements for the degree of
Master of Science in Technology and Policy

Abstract

Light-duty vehicle transportation accounted for 17.2% of US greenhouse gas emissions in 2012 [95]. An important strategy for reducing CO_2 emissions emitted by light-duty vehicles is to reduce per-mile CO_2 emissions. While one approach is to improve vehicle efficiency, greater reductions in emissions can be achieved by switching from gasoline vehicles to electric vehicles, if the electric vehicles run on electricity from clean energy sources.

Batteries affect the consumer adoption of electric vehicles by influencing two important vehicle characteristics: cost and driving range on a single charge. The cost of the battery is a significant fraction of total vehicle cost, and the battery's energy capacity determines driving range. To lower battery costs and improve battery energy capacity, further research is needed. To guide such research, several organizations have created performance targets for batteries, including the Advanced Research Projects Agency-Energy (ARPA-E) and the US Advanced Battery Consortium (US-ABC).

The goal of this thesis is to assess these performance targets based on real-world vehicle performance. A method is developed for estimating the energy requirements of personal vehicle travel, which improves upon previous methods by accounting for per-trip variation of vehicle energy consumption and analyzing data with wider geographic scope. The method consists of a model of battery-to-wheel vehicle energy consumption and a conditional bootstrap procedure for combining GPS travel data with large-scale data from the US National Household Travel Survey.

The research finds that the distribution of energy requirements for US vehicle-trips and vehicle-days (the sum of all trips taken in a day) has a heavy tail, namely that a small proportion of long trips accounts for a disproportionately large amount of energy consumption. Current electric vehicle batteries (2011 Nissan Leaf) can satisfy 83% of vehicle-days, which account for 53% of all energy consumed in personal vehicle travel, while batteries that meet the performance targets can satisfy 98 to 99% of vehicle-days, which account for 90 to 96% of energy. These results allow for a quantification of the benefits of meeting performance targets for battery energy capacity, which can help assess technology readiness and guide allocation of research funding.

Thesis Supervisor: Jessika E. Trancik
Title: Atlantic Richfield Career Development Assistant Professor in Energy Studies

Acknowledgments

This thesis would not have been possible without the support of colleagues, family, and friends. I would especially like to thank:

- Jessika Trancik, for teaching me, for advising my research, and most of all, for pushing me to succeed.
- James McNerney, for your contributions to this work and for our fruitful discussions, which taught me much.
- My TPP classmates, Trancik Lab members, and friends, for helping me survive MIT and feel at home in Cambridge.
- Yin Jin Lee, for your unwavering encouragement.
- Mom, Dad, and Berkeley, for your invaluable perspective and wisdom.

This research was financially supported by an Eni-MITEI Energy Fellowship, the Charles E. Reed Faculty Initiatives Fund, and the New England University Transportation Center at MIT under DOT grant No. DTRT07-G-0001. This thesis is based on collaborative research, the results of which will be published at a later date in a paper [61] that may contain updates to the quantitative results presented here.

THIS PAGE INTENTIONALLY LEFT BLANK

Contents

Chapter 1

Introduction

1.1 Motivation: mitigating the climate impact of transportation

The transportation sector is the second-largest contributor to greenhouse gas emissions in the United States (US), and accounts for a large portion of energy consumption. The US transportation sector accounted for 28% of total greenhouse gas emissions in 2012 [103]. Light-duty vehicles[1] accounted for 57% of these transportation-related emissions, equal to 16% of all US greenhouse gas emissions [95]. As for energy consumption, in 2012, light-duty vehicles accounted for 61% of the all transportation energy consumption in the US [95]. Worldwide, transportation (including air travel) accounted for 27% of final energy consumption [46].

A transition from gasoline-powered to electricity-powered vehicles can reduce emissions from the transportation sector by reducing the carbon intensity of the primary energy sources used. Currently, most vehicles are powered by internal combustion engines, which use gasoline and other petroleum-based fuels. In 2013, petroleum-based fuels accounted for 92% of energy consumed by the US transportation sector [96]. Electric vehicles (EVs) emit zero emissions at the tailpipe, because they operate on electricity from the grid. The only emissions associated with miles driven in an EV are those resulting from generating the electricity consumed and from manufacturing the vehicle. Thus, transitioning from gasoline-powered vehicles to EVs would reduce the carbon intensity of energy used for transportation, if low carbon sources are used for electricity generation [53, 112]. The combination of a cleaner electricity sector and widespread adoption of electricity-powered vehicles is one of the only ways to achieve aggressive emissions reductions in the personal transportation sector [114].

Due to the role that EVs could play in mitigating climate impacts of transportation by displacing gasoline use, many studies have tried to quantify the potential benefit of using them [51]. Depending on the method of analysis, the optimal vehicle technology portfolio for reducing emissions and gasoline use consists of either plug-in hybrids [53] or a combination of EVs and fuel cell vehicles [20]. However, estimating the potential benefit from using EVs is difficult because of the number of

[1] e.g. automobiles, motorcycles, and light trucks under 8,500 lbs

factors involved, such as the availability of charging, the lag in replacing the existing vehicle stock, and the share of vehicle miles traveled that can be supplied by plug-in vehicles [108]. In addition, EV cost-competitiveness is highly sensitive to driving patterns [69]. This thesis contributes to the literature by addressing the variation in EV performance due to driving patterns, which is important for assessing the ability of EVs to meet energy requirements for vehicle travel.

1.2 Research objectives

This thesis poses the question, "are current targets for the energy capacity of EV batteries high enough to meet the demand for travel, based on large datasets on driving habits?" The research focuses on transportation in the US. To answer this question, a method was developed for estimating the energy required for personal vehicle travel that both represents driving patterns in detail and covers a wide scope. The development of the method was the majority of the work for this thesis, and is the core contribution made. The method has two main parts: a model for vehicle tractive energy (amount of energy required at the wheel to move the car, based on drive cycles) and battery-to-wheel efficiency; and a conditional bootstrap procedure for combining detailed GPS data with large-scale cross-sectional travel survey data, from the US National Household Travel Survey. Also, the tendency of rounding trip distance and duration values in travel survey responses is corrected for. Next, a comparison of existing performance targets with the results of the method is presented, followed by a discussion of how an improved understanding of personal vehicle travel can be used to better inform performance targets, policy decisions, and evaluation of electric vehicle battery technology.

The intended audiences for this thesis are people interested in climate change policy or electric vehicle policy, and researchers studying the energy consumption of vehicular travel. Electric vehicle designers may also be interested in this work.

1.3 Thesis structure

The structure of this thesis is as follows. Chapter 2 provides background and a literature review on relevant topics. Chapter 3 describes the data that is used in developing the model and the travel surveys that are studied. Chapter 4 describes in detail the model that was developed to estimate energy requirements of vehicular travel. It has several sections to cover all components of the method and is longer than the others, because the development of the model was a large portion of the work for this thesis. Chapter 5 presents the results generated by the model, and Chapter 6 discusses the results and their relevance to policy. Chapter 7 summarizes the conclusions reached in this research.

This thesis was written by me, with guidance from Professor Trancik. The research contained in this thesis, especially the development of the method, was the result of a collaboration with other members of the Trancik Lab, including Professor Jessika Trancik, James McNerney, and Zach Needell. Much of this work will also be published in a paper at a later date [61], which may contain updates to the quantitative results presented here.

Chapter 2

Background

This chapter provides context for the work presented in this thesis. First, Section 2.1 covers general background information about electric vehicles. Next, in Section 2.2, battery technology is explained in more detail, which will be useful to understand the method development in Chapter 4. Section 2.3 provides an overview of public policies that address electric vehicles, which will provide context for the discussion of performance targets in Chapter 6. Finally, Section 2.4 provides an overview of previous work in this area.

2.1 Electric vehicles

The increased adoption of electric vehicles is one strategy to reduce greenhouse gas emissions and mitigate climate change. This section provides the basic information about electric vehicles needed to understand this topic.

2.1.1 Types of electric vehicles

This subsection presents an overview of electric vehicle technology and the different types of electric vehicles. The distinction between different types of electric vehicles is an important one to make, because a vehicle's source of energy defines its lower limit of possible emissions intensity, and thus its potential to reduce emissions.

Vehicles that can charge their battery from the electricity grid are plug-in electric vehicles (PEV), a category that includes both plug-in hybrid electric vehicles (PHEV) and all-electric vehicles (AEV), also called battery electric vehicles (BEV). Another method of classification is by level of hybridization, which describes the functionality of the electric drivetrain. The general term hybrid electric vehicles (HEV) refers to vehicles with both an internal combustion engine and an electric motor. Some hybrids can run on the electric motor alone, and these are called full hybrids or strong hybrids. In mild hybrids, the electric motor is not strong enough to power the car alone, and instead only provides power to the internal combustion engine in high-demand situations, such as starting the car from a standstill. PHEVs, also known as "range-extended electric vehicles," are strong hybrids with plug-in capability, and are usually designed to run solely on electricity for short driving ranges (up to around 30 miles) and the internal combustion engine for longer ranges. Since PHEVs use two

fuel sources, the optimal design of PHEVs faces complex trade-offs [33]. Collectively, all of these vehicle types are known as electric drive vehicles. All electric drive vehicles can improve efficiency by using regenerative braking, in which braking force is achieved by converting the kinetic energy of the vehicle into charging the battery. Additional detail on the types of electric vehicles and powertrain architectures is available in textbooks [63].

The most commonly used energy storage system for electric drive vehicles is the electrochemical battery. Section 2.2 explains the workings of batteries and the state of the technology. While batteries are the most popular, other forms of energy storage are also being considered, such as fuel cells, ultracapacitors, flywheels, and flow batteries [109, 22].

This thesis focuses on BEVs because of their higher potential to achieve the aggressive emissions reductions goals required to meet climate change mitigation targets, since they run on electricity alone. In addition, the results of the analysis for BEVs would also apply to the capabilities of PHEVs in all-electric mode.

2.1.2 Scalability of electric vehicles

Current adoption levels of electric vehicles are low. In 2013, there were 96,000 plug-in electric vehicles sold in the US, representing around 0.6% of the total vehicle market of 16.5 million vehicles in the US [52]. The two biggest hurdles to the widespread adoption of electric vehicles are cost and driving range, both of which relate to the battery. Other hurdles include the perceived need for public recharging stations, consumer purchasing inertia, and impacts on the electric grid.

The battery is a large portion of the manufacturing cost of an EV, and the battery's energy capacity is the limiting factor for range. For example, an EV's battery can constitute up to half of vehicle production cost, up to $16,000 [34]. Therefore, there is much agreement that innovation in batteries is needed for EVs to become widely used [93, 7, 19]. However, the amount of performance required in different categories is still a topic of debate.

One factor related to the concern about driving range is the availability of public recharging stations. Increased availability of rapid recharging stations in public areas or at workplaces, where EVs can be quickly refueled on-the-go, would effectively increase driving range. More frequent charging would enable greater petroleum displacement by PHEVs, at the cost of faster battery aging [60]. The relative need and utility of charging stations is related to the typical ranges that batteries can provide. Government support may be crucial for successful deployment of charging stations [48].

Consumer purchase patterns are another factor in achieving widespread adoption. Much attention has been given to plug-in hybrids for this reason, because they are palatable to current expectations that one car should be able to satisfy both short- and long-range driving. Understanding market niches may help producers make vehicles more useful. For example, BEVs may be more feasible in suburban areas, due to longer driving distances leading to more customer savings through lower fuel prices, as well as additional room to install charging equipment [82]. Market conditions also influence the rate of deployment of electric vehicles, such as oil prices [13].

The potential widespread use of electric vehicles poses some additional concerns. Large-scale adoption of EVs could run into materials availability issues, specifically for lithium, cobalt, and nickel, which are key components of current batteries [19]. Large-scale and simultaneous charging of vehicles could pose problems for the electric grid [87]. Studies of actual EV customer charging behavior showed a large peak for evening charging at home, with the potential of causing dirtier or less-efficient power plants to come online to meet the demand [80, 49]. However, despite the additional load that electric vehicles impose, they may offer a benefit in acting as storage for the grid, to improve stability and utilization in cases of high penetration of intermittent sources.

2.2 Batteries for electric vehicles

2.2.1 Basics of battery science

While a full explanation of how batteries work is beyond the scope of this text, it is important to highlight here the aspects of battery technology that affect the metrics and targets of interest. Most of the following information comes from the review paper by Cairns [19]. For more details, refer to the original paper, or one of these three textbooks [44, 54, 77].

Batteries are reversible electrochemical systems that function as energy storage devices. Batteries provide energy in the form of electrical charge. Battery capacity is expressed as charge, in units of ampere-hours. A battery's currently stored capacity is often expressed as a fraction of full capacity, and is called "state of charge", or "depth of discharge".

The amount of energy (or charge) that can be extracted from a battery is not a constant quantity. Environmental factors and the speed of discharge can affect the efficiency of the battery pack, effectively changing the amount of energy or charge lost while discharging. These efficiency losses are due to resistances within the battery cell, such as increased crystal formation or side reactions. The general trend is that higher discharge rates correspond to higher internal resistance, and thus lower battery efficiencies. High temperatures can lower the internal resistances, but increase battery aging.

Batteries in practice exist as either small units called battery cells, or larger assemblies called battery packs. For electric vehicle applications, many individual cells are assembled into larger packages called battery packs, in order to create a system with the appropriate amount of energy and power. In creating a battery pack, maintenance systems must be added to ensure proper functioning of all the cells, including mechanical support, electrical connections, controls, and cooling. The total mass of a battery pack is often 50% more than that of the individual cell, to account for these additional support systems.

The ratio of power to energy is sometimes more useful than total power or energy in characterizing batteries, because the power-to-energy ratio is more fundamental to a battery's design. In a battery pack, total power and energy can be increased by simply adding more battery cells of the same design, whereas changing the ratio involves altering the design of the battery cell itself. The ratio of power to energy

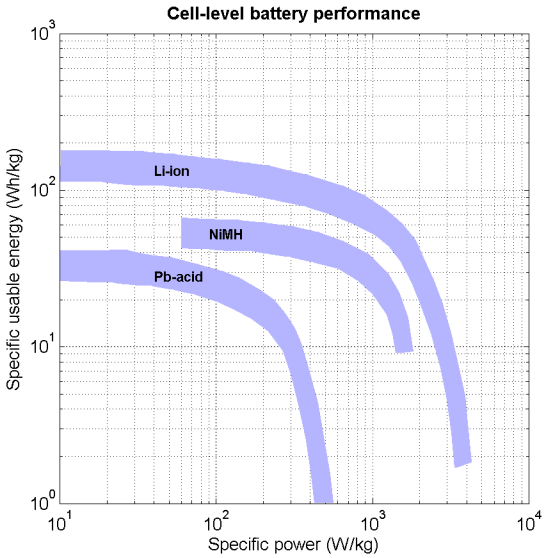

Figure 2-1: Ragone plot of current electric vehicle battery technologies. Data obtained from [86]

is a trade-off faced at the materials and cell design level. For example, the amount of "active material" in a battery determines charge capacity while the amount of "current collectors" determines maximum discharge speed. Therefore, changing the ratio of active material to current collector is one way to tweak the power-to-energy ratio [77]. This is only one of many design choices in designing and optimizing the performance of a battery. The power-energy tradeoff of a battery can be effectively visualized in a Ragone plot.

A Ragone[1] plot describes the performance of an energy storage device in the power-energy plane. An example is shown in Figure 2-1. A single battery corresponds to a curve on the plot, which shows its specific energy at various rates of discharge power. Batteries have a characteristic downward-curving shape, since they produce less energy at higher discharge power. This relationship comes from fundamental physics principles [24, 74]. To be precise, there is no single-answer to "what is the specific energy of this battery?", because the specific energy (and power) depend on how the battery is used [54]. When looking at a plot like this it is important to differentiate between cell-level and system-level performance, since the addition of necessary packing systems to make a full battery may significantly decrease energy density or power density, especially for low-weight technologies [36].

2.2.2 Metrics for battery performance

The previous section explained some fundamentals about how batteries work. This section covers the metrics used to measure battery performance, and the necessary details to interpret them properly.

[1] Named after David V. Ragone, and pronounced "ru-GO-nee".

Specific energy, which is the total energy stored divided by weight of the battery, is the most important metric of battery performance for electric vehicles. It has units of watt-hours per kilogram. A similar metric that is also often used is energy density, which has units of watt-hours per liter. These metrics are useful because they allow comparisons of batteries of different sizes on an equal footing.

Since energy is dependent on how the battery is used, technical metrics for energy must be accompanied by a description of how energy is to be measured. Most metrics specify the measurement of energy under a constant rate of discharge, expressed as a proportion of the battery's total charge capacity C, known as a "C-rate" [77]. For example, for a 60 Ah battery discharging at a rate of C/3 would provide 20 A of current. A rate of 2C would provide 120 A of current. If the capacity of 60 Ah were rated at C/3, then a C/3 rate would last 3 hours, but the 2C rate would last less than 0.5 hours, because of higher inefficiencies at the faster rate.

Specific power and power density are also metrics of interest. Like energy, power ratings are also accompanied by usage descriptions, usually a combination of depth of discharge level and pulse duration. For example, a specific power target might be 400 W/kg for 30 seconds at 80% depth of discharge (20% state of charge).

In addition to energy and power, there are plenty of other important metrics for measuring the value of energy storage. Which metrics are important depends on the application [64]. For electric vehicles, energy is the most important performance requirement, but others are also relevant. These include cost, life, temperature, safety [17]. For example, nickel-cadmium batteries may not be suitable for use in EVs because of cost and toxicity issues [77]. Other relevant metrics include rate of self-discharge, availability of materials, and the need for maintenance. Managing trade-offs between performance in individual metrics is important in battery design, in order to achieve acceptable performance in all metrics.

For batteries to be able to be used in electric vehicles, they need to meet a variety of performance requirements. Designing batteries to meet all performance requirements is constrained by inherent trade-offs between the five main battery attributes: energy, power, cost, longevity, and safety. Meeting one or two of these requirements is easy, but meeting all five at once is difficult. For example, higher power can be achieved through the use of thinner electrodes, but these designs reduce cycle life and safety and increase material and manufacturing costs. In contrast, high energy can be achieved with thicker electrodes that also increase safety and life, but reduce power density [12]. Another such trade-off is that increasing the useable state-of-charge window decreases battery life [59].

2.2.3 State of battery technology

This section provides a brief overview of current and upcoming battery technologies for EVs. Currently, electric vehicles are predominantly powered by either the nickel metal hydride (NiMH) chemistry or lithium-ion (Li-ion) chemistry [19]. NiMH is cheaper on a per-kWh basis than Li-ion, but Li-ion has higher energy density. Thus, NiMH is often used in hybrid vehicles, whereas Li-ion is preferred in PEVs, where the battery capacity needs to be higher. Li-ion cells can be made with a variety of materials for the anode and cathode, with varying advantages in capacity, cycle life, safety, and cost.

Development of new batteries is mainly focused on reducing cost and improving performance, reliability, and life [93]. The main cost drivers for batteries are the high costs of raw materials and materials processing (up to 60%), cell and module packaging, and manufacturing. In addition, the battery for an EV can account for up to two-thirds of the manufacturing cost of the vehicle [114]. Advances in electric vehicle batteries are crucial in reducing the cost of meeting climate targets [16].

Incremental improvements to lithium-ion batteries are mostly focused on innovation in electrode materials and design to improve capacity and voltage. Also important are advances in electrolyte that improve stability, safety, and cycle life. For more details, including a table describing the performance of existing and forthcoming technologies, refer to the US DRIVE Partnership's report [93]. Energy densities may need a two-fold and five-fold increase in order to provide all-electric ranges for PHEVs of 40 to 80 miles and for BEVs of 300 to 400 miles, respectively [88].

In addition to advances in the lithium-ion chemistry, a variety of "beyond lithium" technologies could potentially offer large advances in performance, including lithium-sulfur, magnesium-ion, and sodium-oxygen [107]. Solid-state lithium-ion is another technology that can improve specific energy. Each has its own advantages and obstacles, but these "beyond lithium" technologies could potentially increase energy densities or reduce costs by double or more.

2.3 Public policy addressing electric vehicles

2.3.1 Overview of policies

There currently a number of public policies addressing electric vehicles in the US, both at federal and state levels. This section provides an overview of these policies.

The current US administration has expressed interest in reducing greenhouse gas emissions, and as part of this effort it supports electric vehicles in several ways. In March 2012, the US Department of Energy announced a 10-year vision for PEVs, called the EV Everywhere Grand Challenge, which aims to produce affordable and convenient PEVs by 2022 through supporting battery research and deployment of charging stations [92].

Most of the government support for electric vehicles is through supporting battery research. The DOE spends a significant amount supporting battery research and other research related to electric vehicles. Ability to meet technical performance targets is an important criterion for proposed research projects to receive funding [7]. A detailed overview of these performance targets is provided in Subsection 2.3.2.

Another form of support are government-led demonstration projects, which help accelerate EV deployment by supporting and troubleshooting the early commercialization stages. In 2010, the US General Services Administration procured 116 EVs for use in their own vehicle fleet, providing usage data and increasing EV exposure [105]. In addition, 75% of light-duty vehicle acquisitions must be alternative fuel vehicles, such as plug-in electric vehicles[2]. In 2009, the DOE launched "The EV Project," which provided funding for deploying residential and public charging stations for EVs, to test out business models for EV infrastructure, and collect EV

[2] https://www2.unece.org/wiki/download/attachments/5801244/EVE-05-12e.pdf

usage data [30]. However, the company that won the $99.8 million grant, ECOtality, went bankrupt in 2013, demonstrating that there are still challenges to be overcome in business models for public vehicle charging.

Purchase subsidies and other consumer incentives also play a large role in making EVs more affordable. A federal tax credit of up to $7,500 is available to purchasers or leasers of plug-in vehicles [106]. Many state-level incentives, such as California's Clean Vehicle Rebate Project, also offer rebates for buying or leasing qualified EVs. Other types of incentives include access to carpool lanes when driving alone, such as in California. A database of such state-level incentives is available online [39].

Emissions regulations are another way of using regulatory incentives to support EVs. Electric vehicles, with their high equivalent gas mileage, are at an advantage to help car makers meet US EPA's Corporate Average Fuel Economy (CAFE) standards. At the state level, California's Low Carbon Fuel Standards (LCFS), offers a similar incentive. This policy, which took effect in 2011, set a target of 10% reduction in the carbon intensity of the transportation fuel mix by 2020 - a target which electric vehicles could help meet. However, this policy could be more effective at incentivizing the use of electric vehicles by adjusting some aspects of its implementation [113].

2.3.2 Existing performance targets for electric vehicle batteries

The funding of battery research is a key policy that supports electric vehicles. Performance targets are often used as a key criterion for making funding decisions. This section examines examine existing performance targets for electric vehicles, the organizations that set the targets, and how the targets were chosen.

Performance targets for EV technology describe the desired performance in quantitative terms through specific technical criteria. They specify target categories, such as energy density, power density, lifetime, etc., and a quantitative target for each. The choice of category may vary for depending on either technology or policy applications. Total energy targets are more relevant to designers of vehicles and battery packs, whereas the specific energy targets are more relevant to basic battery research and cell design. There is also a distinction between system-level and cell-level goals. Most organizations include targets for both. Cell-level targets may be more useful for battery researchers, because they are closer to the level of research that they are doing.

This thesis will focus on discussing targets set by organizations in the US, because the US has published the most technically specific performance targets. So far, there are two organizations in the US that publish battery targets: the U.S. Advanced Battery Consortium (USABC) and the Advanced Research Projects Agency-Energy (ARPA-E). The USABC is part of the US Department of Energy's government-industry partnership called US DRIVE, which stands for Driving Research and Innovation for Vehicle efficiency and Energy sustainability[3].

The USABC, formed in 1991, is a team under the US Council for Automotive Research (USCAR) that focuses on energy storage for vehicles, and operates as a partnership between three major US car makers - Ford, Chrysler, and General

[3] `http://www.uscar.org/guest/partnership/1/us-drive`

Motors[4]. They publish a variety of targets for different applications [91]. The set of targets relevant for this work is their EV battery targets [90], and is shown in Table 2-1 and Table 2-2. These EV targets are also used by US DRIVE in planning their research efforts [93]. The USABC's PHEV targets are supported by a published study that uses expert knowledge from industry insiders and standardized test cycles [75]. However, no such study is available for the BEV targets.

In 2010, the Batteries for Electrical Energy Storage in Transportation (BEEST) program of ARPA-E had a Funding Opportunity Announcement that listed several technical requirements, much of it based on USABC's targets. The announcement can be found here [7], and the targets in question can be found on page 13 ("Technical Requirements"). The targets are reproduced in Table 2-1. Meeting the first three targets in the table, relating to energy density and cost, is mandatory to receive funding. ARPA-E has put emphasis on these targets because they are the most important for batteries, as explained earlier.

For both the ARPA-E and USABC, performance targets were used as funding criteria. The USABC targets, being more recent, are more ambitious. However, it is interesting to notice that the requirements for "long-term commercialization" have changed over time, as the targets are revised. In addition, the USABC targets have more technically-detailed categories, likely because USABC is a battery-focused industry group and has more subject area expertise.

In addition to the technical targets described above, high-level targets can be useful as well, such as a target for all-electric range. In 2006, President Bush's State of the Union Address proposed a target of 40 miles of all-electric range for PHEVs, which formed the basis for USABC's technical targets [75]. A target for range has the advantage of being easily evaluated on the basis of consumer utility, which is done by many of the studies covered in Section 2.4. However, they are hard to use to measure technology progress, until converted into technical metrics.

2.3.3 Other uses of performance targets in policy

In addition to their use funding criteria, performance targets can also be used as a communication tool between scientists to develop a research agenda, to coordinate action between organizations, and to measure technology progress to improve accuracy in planning for the future. First, the technical targets can help at the lab bench scale, by helping to communicate the requirements for batteries across scales and fields of research. Detailed technical performance targets could be used as a guide for researchers, and could act as a measure of the downstream utility of upstream technology advances. For example, a lab developing new battery materials could decide whether to focus on improving the energy density or power density of their new material, depending on the size of the shortfall in meeting either performance target.

Secondly, performance targets can be used to aid coordination between different actors, such as between government entities, or government and industry, etc. A simple performance target, such as ARPA-E's \$250/kWh goal, could be used as a way to improve intergovernmental coordination, similar to how a simple cost per

[4]For additional information on the USABC, see [68].

Table 2-1: Performance targets for EV batteries published by ARPA-E's BEEST program in 2010 and USABC in 2013. The first three targets, in bold, are stated as requirements to receive funding from ARPA-E. For comparison, the theoretical maximum specific energy of current lithium-ion technology is 584 Wh/kg, and current state-of-the-art batteries (i.e. Tesla Roadster) have a specific energy of 120 Wh/kg and specific power of 450 W/kg [19].

Target Category	Units	ARPA-E target, 2010 [7]	USABC target, 2013 [90]
Specific Energy Density (at C/3 discharge rate)	Wh/kg	**200 (system), 400 (cell)**	235 (system), 350 (cell)
Volumetric Energy Density (at C/3 discharge rate)	Wh/L	**300 (system), 600 (cell)**	500 (system), 750 (cell)
Useable Energy (at C/3 discharge rate)	kWh	—	45
Cost	$/kWh	**Realistic potential for < 250**	Selling price @ 100,000 units: 125 (system), 100 (cell)
Specific Power Density (30s pulse)	W/kg	400 (system), 800 (cell) at 80% Depth of Discharge	470 (system), 700 (cell) at peak value
Specific Regen Power (10s pulse)	W/kg	—	200 (system), 300 (cell)
Volumetric Power Density (30s pulse)	W/L	600 (system), 1200 (cell) at 80% Depth of Discharge	1000 (system), 1500 (cell) at peak value
Cycle Life	—	1000 cycles at 80% Depth of Discharge, with >20% reduction in any energy/power density metric relative to initial values	1000 Dynamic Stress Test cycles

Table 2-2: Performance targets for EV batteries, continued from Table 2-1

Target Category	Units	ARPA-E target, 2010 [7]	USABC target, 2013 [90]
Round Trip Efficiency	—	80% at C/3 charge and discharge	—
Temperature Tolerance	°C	-30 to 65, with <20% relative degradation of energy density, power density, cycle life and round trip efficiency relative to 25°C performance	-30 to 52
Unassisted Operating at Low Temperature	%	—	> 70% Useable Energy @ C/3 Discharge rate at -20 °C
Survival Temperature Range, 24 Hr	°C	—	-40 to 66
Self Discharge	%/month	< 15 %/month self discharge (of initial specific energy density or volumetric energy density)	< 1 %/month
Safety	—	Tolerant of abusive charging conditions and physical damage without catastrophic failure	—
Calendar Life	years	10	15
Normal Recharge Time	hours	—	< 7 Hours, J1772 charging standard
High Rate Charge	minutes	—	80% ΔSOC in 15 min
Operating Voltage	V	—	220 to 420 (system)
Peak Current (30s Pulse)	A	—	400

	Real-world drive cycles	Pseudo-naturalistic drive cycles	Standardized drive cycles
No energy estimation	[73], [50]		
Simple analytical vehicle model			[20], [10]
Computer simulation	[37], [6]	[14]	[53], [32], [84], [75]
Other	[65]	[55]	

Table 2-3: Vehicle energy estimation methods, for selected papers. The term "pseudo-naturalistic" refers cycles that are modified or synthesized to better represent reality, but are not data recorded from real driving.

energy target was previously used in the DOE's solar energy initiatives [114].

Thirdly, the performance targets provide a benchmark for measuring technological progress and the size of the performance shortfall, which is helpful in policy planning. In the case of EVs, it is crucial to understand the current performance, the desired performance, and the difficulty of bridging gap between the two. Without a proper understanding of technology performance, policymakers would overestimate or underestimate the commercialization barrier, which could mislead policy. The same need applies to hydrogen fuel cell vehicles [57]. Such technology evaluation is important for segmental approaches to climate change policy, by controlling the risk of overshooting climate targets due to technological uncertainty [89].

2.4 Previous studies of vehicle travel and energy consumption

2.4.1 Vehicle per-mile energy consumption

Estimating the per-mile energy consumption of vehicles is an important part of many studies in this research area. In general, creating an estimate of per-mile energy consumption requires two parts: a physics model of vehicle dynamics and a description of vehicle usage patterns, such as drive cycles. Therefore, studies that create their own estimate of energy consumption (either as the goal of the study or as an intermediate step) can be separated along these two dimensions. The drive cycles used to represent vehicle usage paterns can come from naturalistic (real-world) data, pseudo-naturalistic, or standardized cycles, and the physics models range in complexity from the basic physics model [10] to more complicated computer simulations. Table 2-3 shows a few papers along these dimensions. For comparison, the table also includes studies on driving patterns that use GPS data for drive cycles, but do not estimate energy.

While standardized drive cycles are easy to use and are more convenient for others to replicate, they have the drawback of not being representative of real-world driving patterns. In Europe, fuel consumption predictions from standardized drive

cycles in Europe are 21% lower than real-world use, partially because standardized drive cycles fail to represent real-world driving [65]. Another study uses St. Louis GPS dataset of 227 vehicles to estimate PHEV energy consumption with a vehicle simulation called ADVISOR [37]. They compare the performance of their simulated vehicles on the real-world drive cycles with the USA standard drive cycles, and find that gasoline vehicles tend to consume more energy in the real-world cycles than the standardized ones, whereas PHEVs consume less energy in real-world cycles than the standardized ones. Another simulation of electric vehicle design showed that designing a vehicle with the standard UDDS cycle in mind would lead to underperforming in real-world driving [31].

This evidence shows that estimates of energy differ between standardized and real-world drive cycles. Therefore, to make accurate estimates of vehicular energy use, a method based only on standard drive cycles would be inaccurate. Approaches that don't account for the natural variation in travel are not detailed enough to offer insight on the effectiveness of performance targets, since evaluating targets requires higher technical accuracy. However, there is no consensus about how to account for real driving style's impact on energy.

As an alternative to using real-world drive cycles directly, some studies have tried to synthesize their own drive cycles, to overcome the limited availability of real-world cycles. One such study proposes a method to synthesize pseudo-naturalistic drive cycles from real-world drive cycles [55]. Another group of studies have tried to create synthetic drive cycles to aid in estimating vehicle energy usage. One study used road test data to create synthetic drive cycles to infer necessary battery sizes for particular driving ranges [6]. Instead of creating drive cycles, this study used principal component analysis to identify characteristics of standard drive cycles that impact energy consumption to circumvent the need for naturalistic drive cycles in designing power control strategies [32]. Another study uses statistical techniques to generate synthetic drive cycles from real ones [56].

2.4.2 Applications of understanding energy consumption

There are a variety of purposes why an understanding of the energy consumption of vehicles is useful. This section gives an overview of the various applications, but due to the breadth of applications, this list is not exhaustive.

One goal of studying vehicle energy consumption is to understand the factors that influence it, which can inform strategies for reducing energy use. Analyses of vehicle energy consumption based on drive cycles suggest that changes to traffic policy and human behavior can reduce vehicular energy consumption [9]. In particular, reducing accelerations and cruising speeds can reduce fuel consumption [14].

Energy consumption analyses can also be used to evaluate and compare vehicle technologies. For example, variation in how vehicles are used can affect the rank order of primary energy consumption for alternative vehicle technologies [20]. Energy consumption is also an important factor in designing PHEVs for maximum petroleum savings [84], designing battery size [6], designing an ideal all-electric range for PHEVs [84, 108], or modeling battery degradation during vehicle use [56]. In addition, the economic and environmental benefits of EVs vary substantially when calculated under different drive cycles, suggesting that a segmented approach (e.g.

separating urban drivers from highway drivers) for marketing EVs and considering policy impacts may be more effective [47].

2.4.3 Studies of driving patterns

Another body of work studies the performance of EVs and PHEVs on the basis on driven distance alone, without accounting for the energy needed to meet those driving ranges. Several papers have studied the feasibility of EVs and PHEVs to meet travel demands by studying the proportion of travel needs met with limited range vehicles, based on distances traveled in current driving patterns [50, 73]. These studies focus on distance only, without relating it to the necessary energy capacity of the batteries. Both of these studies are similar. They are both based on longitudinal GPS data, which has a small vehicle sample size (255 and 484), but follow their subjects for a whole year. They try to segment the market by studying the number of times trip distance exceeds a certain amount. For example, a 100-mile range EV could meet the needs of 17% of drivers if adaptations were made for 2 trips longer than 100-miles, and 32% of drivers if adaptations were made 6 times a year [73]. Also, a 100-mile range BEV would meet the needs of 50% of one-vehicle households and 80% of multiple-vehicle households [50]. However, these papers treat the technology like a black box, and do not address the question of how much EV battery capacity is needed to provide for the given driving ranges.

Many studies have focused on the potential to replace miles driven with a finite all-electric range and limited charging [108]. This study makes the simplifying assumption that PHEVs that are powerful enough to drive in pure electric mode under all driving conditions, instead of directly calculating power and energy requirements.

Although many studies do not address the question of energy requirements, the methods they use are useful, because data on miles driven is more readily available and easier to collect. However, their results have the drawback of high sensitivity to assumptions about vehicle energy consumption and driving patterns. In PHEVs, the battery capacity defines the threshold between zero tailpipe emissions and using gasoline. Since usable battery capacity depends on how the vehicle is driven, the climate mitigation potential of PHEVs are particularly sensitive to driving patterns. Therefore, estimating energy consumption accurately and accounting for real driving patterns are even more important.

THIS PAGE INTENTIONALLY LEFT BLANK

Chapter 3

Data

This chapter provides an overview of the data that will be used as inputs to the model and the analysis. The first section covers the three types of data required for the model: drive cycles from GPS-based travel surveys, vehicle specifications, and fuel economy measurements. The second section describes the 2009 National Household Travel Survey, which provides data on travel patterns and is the focus of the analysis for the thesis.

3.1 Model parameters

3.1.1 Drive cycles from GPS-based travel surveys

Detailed data on personal vehicle travel from a GPS-based travel survey is used. The data field of particular interest is the "drive cycle" of typical vehicle trips. The drive cycle, sometimes called driving cycle, is a record of the vehicle's instantaneous speed at regular intervals throughout the duration of trip. This detailed data allows us to estimate the energy consumed during the trip. For each trip, the travel survey also provides other information, such as time of day, demographic information about the survey respondent, etc.

The GPS-enabled travel survey used is from the 2010-2012 California Household Travel Survey, conducted by the California Department of Transportation. This dataset is available for free from the National Renewable Energy Laboratory's (NREL) Transportation Secure Data Center website [67]. The survey's GPS subsample contained 2,908 vehicles with 65,623 vehicle trips. For each vehicle, data was collected for 7 days. The speeds in the drive cycles were measured at a rate of 1 Hz, or every second. The data used is not the raw GPS data, but a cleaned version that NREL processed with a data filtering algorithm to filter out errors, such as unrealistic speeds, and to interpolate for missing data. More information on the data filtering process can be found here [29, 18].

The sampling rate can be a point of concern for GPS data. The data used for this analysis is measured in 1 second intervals, but one might ask, "is this sampling frequency high enough?" While this question is not directly answered in the analysis, data with 1 Hz sampling frequency should adequately represent reality because typical driving events (e.g. accelerations) last longer than 1 second and would be

well approximated by 1 Hz data.

Another point of concern is differences in driving habits between regions. Since only the California dataset is used, these regional differences would not be observable in our analysis. There are some other GPS-based travel surveys from Texas and Atlanta, which are also available on NREL's website, but the California dataset was chosen because it is the most up-to-date and is of higher quality than the other ones. Regional differences in driving would only impact the model if trips of the same distance and duration had different energy consumption between regions. Different regions would be expected to have different distributions of trip distance and trip durations, but this in itself would not impact the results, for reasons explained in Chapter 4.

3.1.2 Vehicle specifications

The proposed method for estimating a vehicle's energy requirement for a trip requires knowing its specifications, such as mass and air drag coefficient. The analysis in this thesis focuses on only one vehicle model, the 2011 Nissan Leaf. It was chosen because it has been the highest selling BEV in the US for the last 3 years [45], with the runner-up being the Tesla Model S. The Leaf was the first BEV that was designed to be affordable, in the hopes of wider adoption, so it is appropriate to use because the analysis will make conclusions about increasing EV adoption.

The vehicle specifications for the 2011 Nissan Leaf that are relevant to the model are shown in Table 3-1. Official Nissan sources don't provide all of the data required for the method, so other sources must be used for certain parameters. The sources used were: 2011 Europe Nissan Leaf Technical Data [71]; a blog post that cites Nissan Leaf specifications [25]; a vehicle design textbook, for a typical value of rolling resistance for passenger cars on concrete [35]; EPA fuel economy data [101]; news sources [81, 110]; and a Nissan Leaf First Responder's guide [70]. Dynamometer coefficients are obtained from the EPA Test Car data website [99], which contains data that is mostly provided by automobile manufacturers.

3.1.3 EPA fuel economy measurements

Vehicle fuel economy is used in the model to help estimate vehicle efficiency, as well as to validate aspects of the model. The fuel economy data used is published by the US Environmental Protection Agency (EPA), available online [101]. The EPA's fuel economy data is obtained from either in-house EPA measurements or from verified manufacturer tests [97]. The testing procedure uses dynamometers to simulate driving in a controlled environment [98]. The dataset also contains other useful information, such as all-electric range and electric motor power.

This dataset provides the fuel economy of the 2011 Nissan Leaf, the vehicle of used in the model. Fuel economy for electric vehicles is expressed either in terms of mileage (miles per gallon equivalent) or as energy consumption (kilowatt-hours per mile). These values are calculated from the amount of electricity used to recharge the vehicle after a test run. The EPA follows the SAE J1634 standard procedure for measuring BEV fuel economy with AC recharging [4]. While SAE J1634 provides standard procedures for measuring BEV fuel economy via both AC recharging energy

Table 3-1: 2011 Nissan Leaf vehicle specifications.

Parameter	Value	Source
curb weight (m)	1,525 kg	[25, 71]
rolling resistance (μ_{rr})	0.015 (passenger car on concrete)	[35]
frontal area (A)	2.27 m^2	[25]
drag coefficient (C_d)	0.29	[25, 71]
motor power	80 kW	[25, 71]
motor max torque	280 Nm	[25, 71]
motor type	AC synchronous	[25, 71]
transmission	single speed gear reduction, 7.9377	[25, 71]
tire size	P205/55R16	[25, 71]
battery capacity	24 kWh	[25, 71]
battery voltage	345 V	[25, 71]
battery pack weight	648 lbs (294 kg)	[70]
battery weight, cells only	171 kg	[derived]
specific energy of cells	140 Wh/kg	[81, 110]
battery type	laminated lithium-ion	[25, 71]
EPA all-electric range	73 miles	[101]
unadjusted city mileage	151.5 MPGe	[101]
unadjusted highway mileage	131.3 MPGe	[101]
dynamometer coefficient, A	33.78 lbf	[99]
dynamometer coefficient, B	0.0618 lbf/mph	[99]
dynamometer coefficient, C	0.02282 lbf/mphÂš	[99]
dynamometer test weight	3750 lbs	[99]

and DC discharge energy, the EPA uses only the former method because the latter is expensive to implement.

The EPA publishes two sets of fuel economy measurements, adjusted and unadjusted. The unadjusted values are the raw measurements from the vehicle tests, while the adjusted fuel economy has been shifted downward to represent the more demanding driving conditions experienced in real life. This adjusted fuel economy is the official EPA rating for vehicles. The adjustment is made using a prescribed formula, called the "derived 5-cycle adjustment method", which has a maximum value of 30% [4]. The rules for this adjustment procedure, and EPA fuel economy labeling in general, can be found in the Code of Federal Regulations (CFR) [2, 3, 1] and an EPA report [100].

An alternate source for fuel economy measurements is the EPA Test Car dataset [99], which contains individual results for the different EPA test procedures, with data mostly provided by manufacturers. This research uses the first dataset because its data matches to the official fuel economy ratings that appear on the EPA window sticker for new vehicles.

3.2 US National Household Travel Survey

The data that will be studied with the model and used to produce the primary results is the 2009 US National Household Travel Survey (NHTS). The NHTS is a large cross-sectional dataset about all modes of travel in the United States, with a sample size of 150,147 households and 740,846 automobile trips. This is a large travel survey in the U.S. conducted by the Federal Highway Administration, in which the respondents record their trips over a 24-hour period. Data is collected over an entire year, and from all regions of the US. Characteristics for each trip entry include trip distance, duration, mode, and other demographic variables such as household income or population density of the area. The data is available online [104].

Chapter 4

Model Development

For this thesis, a model was developed to calculate the distribution of requirements for battery energy capacity, based on cross-sectional travel survey data, for a given vehicle. This chapter describes how the model works, how it was developed, the decisions made, and why it is appropriate for the analysis in this thesis.

To explain how the model calculates a distribution of battery energy requirements, this chapter walks through the modules in the model in increasing level of abstraction, starting from the most physical level, a single trip. This overall flow of the model is illustrated in Figure 4-1. The first step in the model is to pick a vehicle. For the analyses in this thesis, the vehicle used is the 2011 Nissan Leaf, an all-electric vehicle. Next, the model looks at a single vehicle-trip. If the second-by-second speed achieved over the trip is known, physical principles can be used to calculate the energy required at the wheels for the chosen vehicle to follow the same trip, explained in Section 4.1. Next, an understanding of vehicle efficiency is used to find the energy required from the battery to provide for the energy at the wheels, i.e. tank-to-wheel efficiency, in Section 4.2. However, the NHTS data does not contain the second-by-second speed data necessary for this procedure to be carried out. To solve this, a conditional bootstrap procedure is developed in Section 4.3 that intelligently finds matching GPS trips, which contain speed data, for each NHTS trip, effectively combining the strength of both datasets. Each of the following sections also validates its part of the method.

4.1 Tractive energy requirements of trips

This section discusses the most physical level of the model: calculation of tractive energy for a trip. First, the definition of tractive energy is given, followed by the formula used to calculate it, and a brief discussion of its physical interpretation. The goal of this part of the model is to calculate the tractive energy requirement of a given drive cycle for a vehicle.

4.1.1 Definition of tractive energy

Before defining tractive energy, other definitions must first be clarified. The term "powertrain" refers to the components of a vehicle that generate power and deliver it

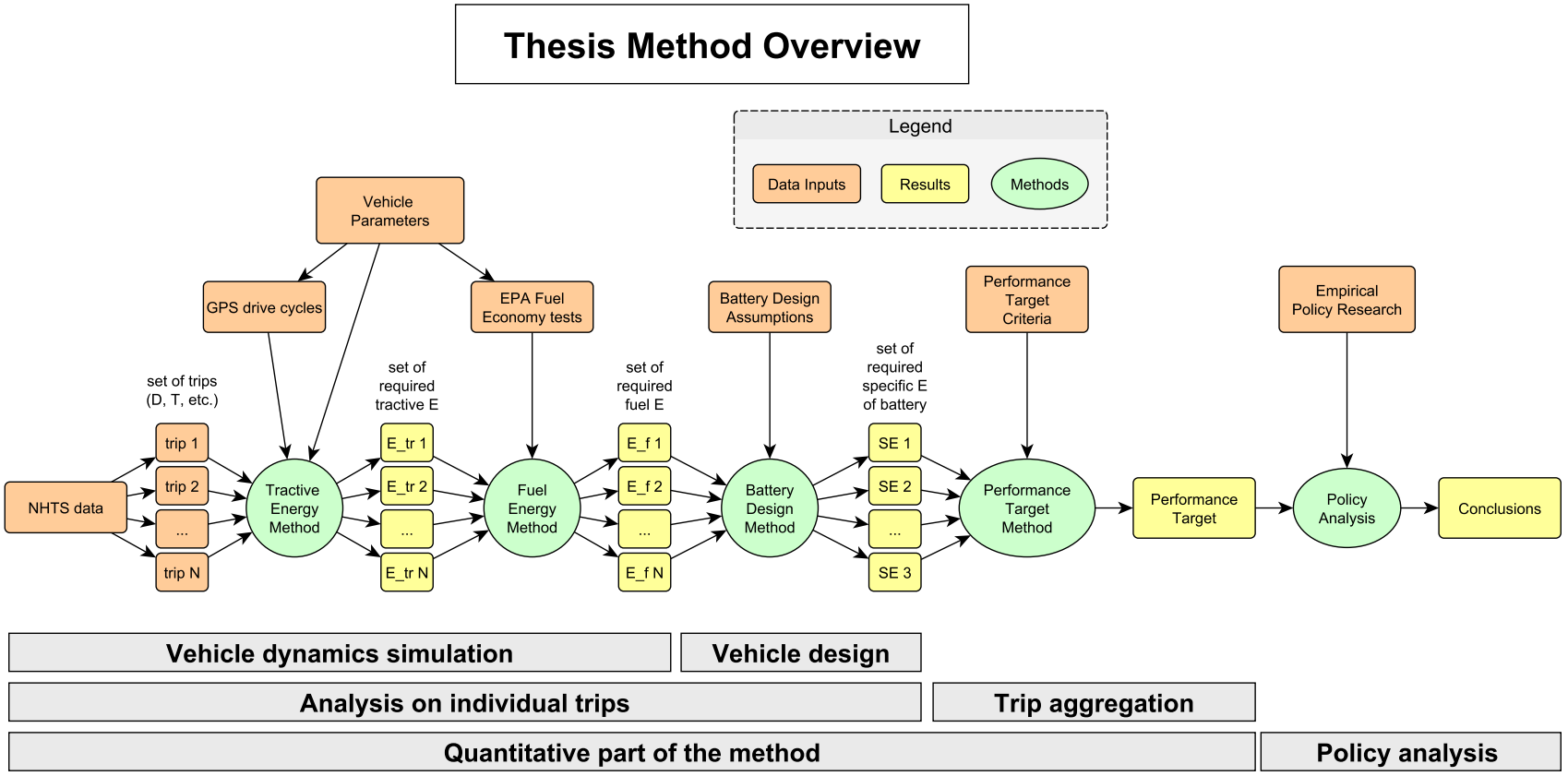

Figure 4-1: Graphical depiction of overall model and method

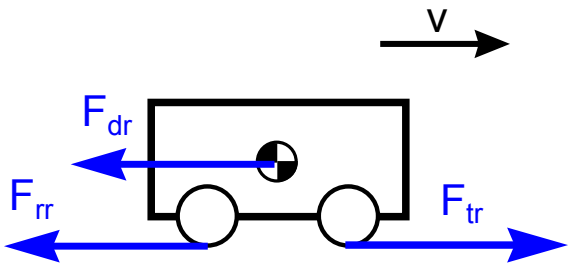

Figure 4-2: Free-body diagram of longitudinal forces on a vehicle body in forward motion, on level ground and in stationary air

to the road surface. For an electric vehicle, this includes the battery, motor controller, traction motor, drive shafts, and wheels. A "drive cycle" is a series of data points that record the speed of a vehicle over time, for a vehicle-trip.

The definition of tractive energy begins with tractive force. Tractive force, also sometimes referred to as tractive effort, is defined as the force propelling the vehicle forward, transmitted to the ground through the drive wheels [54, 35]. Tractive power is tractive force multiplied by the velocity of the vehicle: $P_{tr} = F_{tr}v$. Tractive energy of a trip is the integral of tractive power over the duration of a trip, the details of which will be covered in the next section. Thus, tractive energy describes the amount of energy required at the wheels for the vehicle to follow the given driven cycle. Note that this is a separate quantity from the amount of fuel energy consumed during the trip. Tractive energy can be aggregated over various vehicle-trips and vehicle-days, to give an estimate of the amount of energy required in personal vehicle travel.

Tractive energy is a useful quantity to analyze because it is independent of the technology used to propel the vehicle. As explained in the next section, it only depends on the drive cycle and the bulk characteristics of the vehicle (mass, rolling resistance, and air drag coefficient). This property makes tractive energy a useful metric when comparing the performance of different technologies, because it largely separates the impact on total energy arising from the drive cycle versus from the propulsion technology used.

4.1.2 Physical model of tractive energy

To help explain the origin of tractive energy, this section builds up a physical model for tractive energy from first principles. Using the free-body diagram of the force on a vehicle shown in Figure 4-2, the net force on a vehicle under forward motion can be written as:

$$F_{net} = F_{tr} - F_{rr} - F_{dr}$$

where F_{tr} is the tractive force exerted by the car's powertrain (positive if accelerating, negative if braking), F_{rr} is the rolling resistance force, and F_{dr} is the drag force. Note that this formulation ignores the hill-climbing force associated with changes in elevation. This formulation is a common way to create a simple model for the forces on a vehicle [58, 54]. The textbook by Gillespie [35] offers more details

on the origins of these vehicle dynamics forces.

Using Newton's first law, the net force on the vehicle can be replaced by mass times acceleration:

$$(1+q)ma = F_{tr} - F_{rr} - F_{dr}$$

The $(1+q)$ factor is added to represent rotational inertia in the vehicle, i.e. that some amount of force is necessary to make the rotating parts of the car rotate faster when the vehicle accelerates linearly. Most of this force is absorbed into the angular momentum of the electric motor, which has high angular speeds.

The above equation can be rewritten to solve for the required tractive force, if the drag force, rolling resistance force, and the acceleration of the vehicle are known:

$$\begin{aligned} F_{tr} &= (1+q)ma + F_{rr} + F_{dr} \\ F_{tr} &= (1+q)ma + \mu_{rr}mg + \frac{1}{2}\rho A C_d v^2 \end{aligned}$$

The standard formulations for the rolling resistance and air drag forces have been used. The coefficient of rolling resistance μ_{rr} can be coarsely approximated with a constant value, or modeled with a functional form that depends on velocity and other vehicle conditions, as in SAE J2452[1] [38]. For empirical values of the parameters for the 2011 Nissan Leaf, see Table 3-1 in Chapter 3.

To calculate the total amount of energy exerted by the powertrain over a given driving cycle, the instantaneous power delivered by the powertrain must be calculated, and then integrated over the entire drive cycle:

$$\begin{aligned} P_{tr} &= \left[F_{tr}\right]_+ v \\ &= \left[(1+q)ma + \mu_{rr}mg + \frac{1}{2}\rho A C_d v^2\right]_+ v \\ E_{tr} &= \int_{drive\,cycle} \left[(1+q)ma + \mu_{rr}mg + \frac{1}{2}\rho A C_d v^2\right]_+ v \, \mathrm{d}t \end{aligned}$$

The notation $\left[F_{tr}\right]_+$ means to evaluate the expression inside the bracket only when it is positive, and set the expression equal to 0 if it is negative. This is important to include because only the energy expended by the powertrain should be counted towards the tractive energy requirement, and not the energy lost to the brakes (i.e. during negative tractive force). Energy recovered through regenerative braking and spent for auxiliary uses (HVAC, lights, etc.) are accounted for in powertrain efficiency, described in a later section.

To give a physical sense of the interaction of the terms in the tractive power equation, the equation can be related to several physical regimes of vehicle operation. Vehicle operation can be split into 3 different regimes, as described by An and Ross [10]. The regimes are (1) "acceleration", where vehicle acceleration is positive and tractive force is positive; (2) "powered deceleration", where acceleration is negative but tractive force is positive; and (3) "braking", where acceleration and tractive

[1] "Stepwise Coastdown Methodology for Measuring Tire Rolling Resistance", `http://standards.sae.org/j2452_199906/`

force are negative. Intermediate regimes can be defined as well: "cruising", where acceleration is 0 and tractive force is positive; and "coasting", where acceleration is negative and tractive force is 0. These regimes are highlighted in several sample drive cycles from the California GPS dataset in Figure 4-3. Note that powered deceleration (blue dots) occurs more often while cruising at highway speeds.

4.1.3 Empirical formula for tractive energy

In the model used for this thesis, an empirical model is used to calculate tractive energy. This model is known as the dynamometer road load equation, which uses three coefficients (A, B, and C) that are obtained from empirical testing of vehicles under standardized conditions. The previous physical model was presented as a comparison, to help with physical interpretation of the empirical model presented here. Previous studies of vehicle energy consumption have also used this empirical formulation [58, 42, 66].

Instead of building a model of road load from first principles, an empirical relationship is used. Road load is defined as the sum of aerodynamic drag and rolling resistance forces. Road load, as a function of vehicle speed, can be determined empirically through a procedure called "coastdown testing"[2]. The coastdown test consists of driving a car up to a high speed, such as 80 MPH, and letting it coast down to a low speed in neutral gear while recording the vehicle's speed over time. The resulting trace of velocity can be used to find instantaneous acceleration, which is used to find instantaneous force at each speed, which gives the road load. The road load relationship is fit with a regression, using the following form:

$$\begin{aligned} \text{Road load} &= F_{drag} + F_{rr} \\ &= A + Bv + Cv^2 \end{aligned}$$

The original purpose of obtaining these coastdown coefficients is to calibrate dynamometers to accurately reproduce the road load of vehicles. The EPA publishes coastdown coefficients for all commercially-produced vehicles in their Test Car data files [99]. These coefficients are usually measured by the manufacturer, using the Society of Automotive Engineers's (SAE) standardized procedure for coastdown testing, SAE J1263[3]. In the Test Car data files, the EPA publishes two sets of ABC coefficients, called "target" and "set". The "target" coefficients refer to coefficients that fit the coastdown data, while the "set" coefficients are adjusted values of the "target" coefficients that are inputted to the chassis dynamometer to reproduce the same road load as in the coastdown test. For the purposes of this work, "target" coefficients are used.

Using this formula for road load, the tractive energy for a drive cycle can be calculated by using a similar formulation as above, but replacing the physical air drag and rolling resistance terms with the empirical form using the A, B, and C coefficients. Tractive energy becomes

[2] `https://hyundaimpginfo.com/resources/details/coastdown-facts/`

[3] `http://www1.eere.energy.gov/vehiclesandfuels/avta/pdfs/hev/htp001r2.pdf` and `http://standards.sae.org/j1263_201003/`

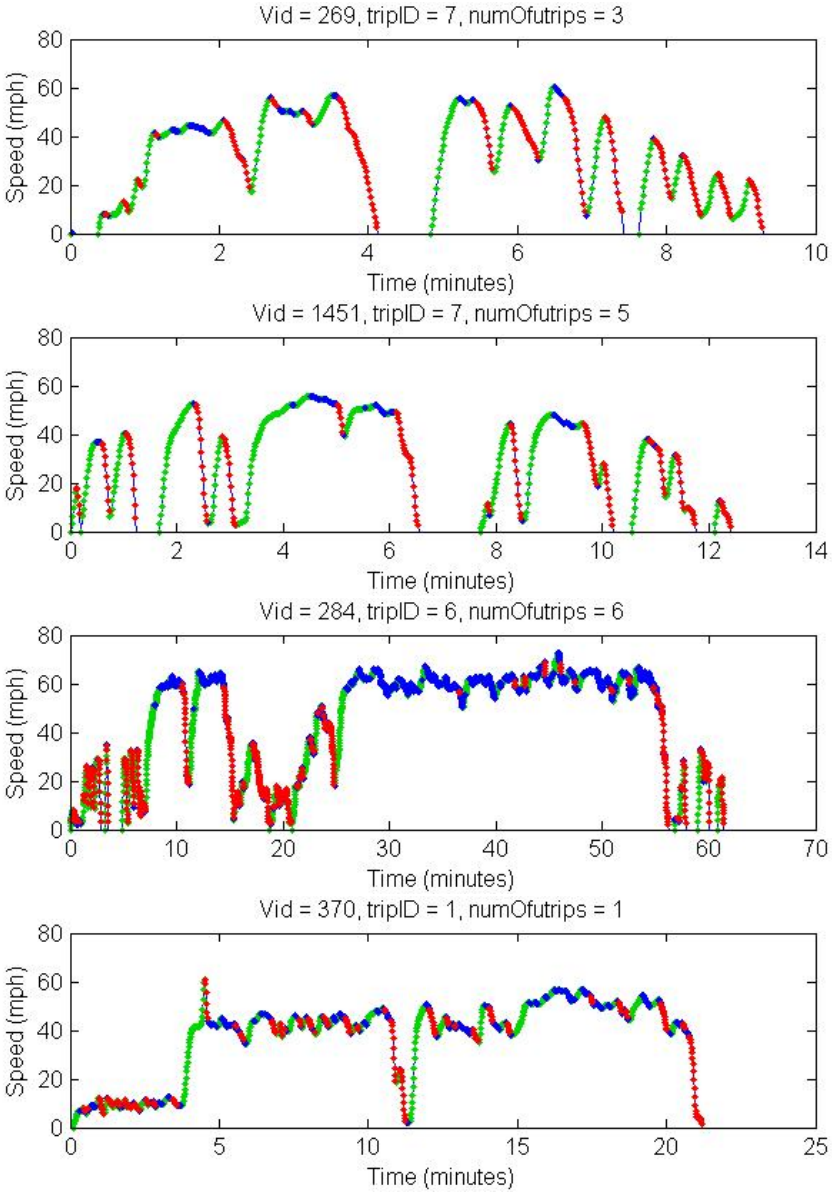

Figure 4-3: Sample drive cycles from the California GPS dataset. The three driving regimes are highlighted colors: acceleration (green), powered deceleration (blue), and braking (red).

Table 4-1: Dynamometer coefficients for the 2011 Nissan Leaf. Source: EPA Test Car list data [99]

A coefficient	33.78 lbf
B coefficient	0.0618 lbf/mph
C coefficient	0.02282 lbf/mph^2

$$E_{tr} = \int_{drive\,cycle} \left[(1+q)ma + A + Bv + Cv^2\right]_+ v \, \mathrm{d}t$$

The values of the A, B, and C coefficients can be interpreted according to the corresponding functional form from the physical model. As described in the Code of Federal Regulations[4], the A coefficient represents the constant friction term, the B coefficient represents road load from drag and rolling resistance, which are a function of vehicle speed, and the C coefficient represents aerodynamic effects, which are a function of vehicle speed squared. The values of the dynamometer coefficients used for the 2011 Nissan Leaf are shown in Table 4-1.

Note that this has an additional term that depends linearly on velocity, which seems to be absent from the theoretical formulation above. The linear term corresponds to the velocity-dependent component of rolling resistance, and to the drag in the powertrain (e.g. friction in bearings). At low speeds, the coefficient of rolling resistance changes linearly with speed, but at higher speeds it changes with the square of speed, or speed to the 2.5 power, depending on vehicle and wheel type [35, 76]. Rolling resistance also depends on the level of tire inflation. Powertrain losses may also be linear with speed because of viscous drag, e.g. oil in the wheel bearings [76].

4.2 Powertrain efficiency and battery energy

Next, an estimate for powertrain efficiency is developed, which will enable calculation of the battery energy requirement from the tractive energy requirement. There are many aspects of estimating powertrain efficiency, and developing an accurate estimate requires careful consideration of how vehicle performance varies under different conditions and how battery energy behaves.

This section first defines powertrain efficiency, explains how it is calculated with GPS data and EPA fuel economy data, and finally validates the choice of method and resulting value for efficiency. The value for the powertrain efficiency of the 2011 Nissan Leaf is shown in Table 4-2, along with intermediate steps used in the calculation.

[4] 40 CFR 1066.210(1)(d). Accessed at `http://cfr.regstoday.com/40cfr1066.aspx#40_CFR_1066p210`

Table 4-2: 2011 Nissan Leaf cycle-averaged powertrain efficiency, with intermediate steps used in the calculation

55% city / 45% highway combined fuel economy	99 MPGe
Battery charger efficiency	90%
Total distance of all GPS trips	6.4021×10^5 miles
Total tractive energy requirement of all GPS trips	7.4829×10^{11} J
Cycle-averaged powertrain efficiency	106.20%

4.2.1 Definition of powertrain efficiency

The engineering definition of instantaneous powertrain efficiency (PTE) is defined as the ratio of the tractive power (power transferred from the wheels to the road) to the power being drained out of the battery.

$$\text{instantaneous PTE} = \frac{\text{tractive power}}{\text{power drained out of battery}}$$

This efficiency accounts for the energy lost in the physical processes that connect the stored energy in the battery with the work done by the wheels to move the vehicle. This instantaneous powertrain efficiency varies with operating condition (e.g. motor torque and rpm, battery discharge power), and so this will vary over the course of a given drive cycle.

Building off of this definition, average powertrain efficiency for a given drive cycle can be defined as:

$$[\text{average PTE}]_{drive\,cycle} = \frac{[\text{tractive energy required}]_{drive\,cycle}}{[\text{energy drained out of battery}]_{drive\,cycle}} \tag{4.1}$$

By definition, average powertrain efficiency relates the actual energy drained from the battery over a drive cycle with the tractive energy requirement defined in the previous section. This average powertrain efficiency also varies between different drive cycles. However, it is difficult to use this definition to calculate a different powertrain efficiency for each drive cycle, because of the difficulty in estimating the actual battery energy spent for a particular drive cycle.

Instead, powertrain efficiency is further aggregated into a single value to be used for all drive cycles. This is labeled as the "cycle-averaged powertrain efficiency", and it represents the average powertrain efficiency across drive cycles normally experienced in real-world driving:

$$\text{cycle-averaged PTE} = \frac{\text{average per-mile tractive energy spent in real-world driving}}{\text{average per-mile battery energy spent in real-world driving}}$$

It is important to note that powertrain efficiency, defined this way, can be greater than 1 for vehicles with regenerative braking. Ott et. al proposes an alternate definition of powertrain efficiency that addresses this issue and stays between 0 and 1, retaining the traditional meaning of efficiency [72]. However, the definition proposed above is suitable for our purposes, because our method only requires some representation of the relationship between tractive energy and battery energy.

The above definition of powertrain efficiency accounts for regenerative braking, but other studies have suggested alternative methods that account for regenerative braking separately from powertrain efficiency [15, 26, 43]. A possible advantage of separating the two is to reduce the variation with respect to drive cycle for both powertrain efficiency and regenerative braking efficiency [72]. Estimates of the fraction of kinetic energy that is recoverable through regenerative braking range from 15% to 30% on standardized cycles, or to 50% for buses [77], while others claim the limit is 40% [54].

4.2.2 Calculation of cycle-averaged powertrain efficiency

To calculate a value for cycle-averaged powertrain efficiency, the following equation is used, based on the above definition:

$$\text{cycle-averaged PTE} = \frac{\overline{EPM}_{tr,GPS}}{\overline{EPM}_{batt,EPA}}$$

where $\bar{EPM}_{tr,GPS}$ is the average per-mile tractive energy of trips in the GPS dataset, and $\bar{EPM}_{batt,EPA}$ is the EPA's estimate of the average per-mile battery energy spent in real-world driving. By using this value, the total battery energy spent in the GPS cycles is equal to the total tractive energy spent in the GPS cycles multiplied by the EPA's MPG estimate.

The value of $\bar{EPM}_{batt,EPA}$ is EPA's combined MPG value. While the MPG values were calculated from specific city and highway drive cycles, the EPA's adjustment makes these MPG values representative of real-world driving. By using this data for the calculation, the value of powertrain efficiency will be inherently representative of real-world drive cycles, because the GPS trips represent real-world drive cycles, and the EPA's adjusted MPG value is the best approximation available of the true MPG value over real-world drive cycles and real-world driving conditions.

Calculating average per-mile tractive energy of real-world trips. The model for tractive energy based on the dynamometer coefficients is used to calculate the average tractive energy per mile required for the GPS trips. For each trip in the GPS dataset, the tractive energy requirement is calculated. Tractive energy is then summed up for all trips in the GPS dataset and divided by the total distance traveled to find the average tractive energy. This is the formula:

$$\overline{EPM}_{tr,GPS} = \frac{\sum_i E_{tr,i}}{\sum_i D_i}$$

where the sums are over all trips i in the GPS dataset.

Calculating average per-mile battery energy of real-world trips. The denominator used is based on the combined MPG value from EPA, but a few corrections to the published value must first be made. The formula used for the average energy-per-mile required from the battery based on EPA data is

$$\overline{EPM}_{batt,EPA} = \eta_{charge} \times \rho_{gasoline} \times \text{MPGe}^{-1}_{combined}$$

where the battery charging efficiency is $\eta_{charge} = 0.9$ and the energy content of gasoline[5] is $\rho_{gasoline} = 33.7\,^{\text{kWh}}/_{\text{gallon}}$. The combined fuel economy in miles-per-gallon-equivalent (MPGe) is a harmonic average of the city and highway assuming 55% and 45% driving shares, respectively, following the same formula that the EPA uses[6]:

$$\text{MPGe}_{combined} = \left(\frac{0.55}{\text{MPGe}_{city}} + \frac{0.45}{\text{MPGe}_{hwy}} \right)^{-1}$$

The combined miles-per-gallon-equivalent fuel economy is meant to represent real-world driving, which is assumed to have a mix of 55% city driving and 45% highway driving.

The origin of the EPA's published MPGe values makes these adjustments necessary. The EPA's measurement of energy consumption is the amount of electricity used to recharge a vehicle after performing dynamometer tests[7] of standardized drive cycles until the battery runs out of energy [4]. The two drive cycles used are the "Federal Test Procedure" (FTP) cycle, which represents city driving, and the "Highway Fuel Economy Test" cycle, which represents highway driving. The two drive cycles can obtained from the EPA Dynamometer Drive Schedules website[8].

The EPA converts the raw measurements of energy consumption to MPGe values using $\rho_{gasoline}$ as the conversion factor and labels the results "unadjusted fuel economy." These are then adjusted downward (by a maximum of 30%) to represent performance under real-world driving conditions[9]. Further details in converting EPA-reported MPG values to actual in-use MPG can be found in the EIA's report on their method for estimating fuel consumption in the 2009 NHTS, which includes correcting for regional factors like geography [94].

Because the reported energy consumption is based on the energy required from the wall socket to recharge the battery, the reported energy consumption or fuel economy numbers includes the efficiency of the battery charger. These "wall-to-vehicle" losses are assumed to be 10%, the same as in EPA's calculations of the emissions impact of electric vehicles [102]. Therefore, the reported energy consumption numbers are multiplied by 0.9. Other studies estimate that charging efficiency ranges from around 80% [62] to 94% [26].

[5] `http://www.fueleconomy.gov/feg/evsbs.shtml`

[6] `http://www.epa.gov/fueleconomy/documents/420f14015.pdf`

[7] The SAE J2264 standard is used for dynamometer test procedures, available at `http://standards.sae.org/j2264_201401/`. The procedures are also described in 40 CFR 1066, available at `http://cfr.regstoday.com/40cfr1066.aspx#40_CFR_1066`

[8] `http://www.epa.gov/nvfel/testing/dynamometer.htm`

[9] More information about EPA procedures can be found at `http://www.epa.gov/otaq/carlabel/regulations.htm`

Assumptions made in this method. The proposed definition of powertrain efficiency makes a few assumptions that may affect its accuracy. The calculated powertrain efficiency is calibrated by the EPA's adjusted estimates of fuel consumption, which are assumed to represent real-world driving. The GPS drive cycles are assumed to be unbiased and representative of real-world driving as well. In addition, auxiliary power consumption is included as part of powertrain efficiency, and not treated separately. Imperfect data about the trips limits how accurately powertrain efficiency can be calculated. Many factors that impact powertrain efficiency are unknown, such as ambient temperature (especially important for EV batteries), vehicle temperature at the start of the trip, and weight of passengers and cargo (although mass may have a small effect [21]).

4.2.3 Powertrain efficiency validation

To double-check the calculated value for powertrain efficiency of the 2011 Nissan Leaf, it is compared to those found in the literature. The definition of powertrain efficiency used here is often referred to as "tank-to-wheel" efficiency in the life-cycle assessment literature, and is usually close to 80% for battery electric vehicles [112, 40, 41, 27, 20]. A greater range of powertrain efficiency values are reported by other sources. These include 88% for the Tesla Roadster[10], a BEV; 71% for Li-ion vehicles, based on component-wise efficiency estimates [8]; or a range of 55% to 92%, depending on HVAC usage and ambient temperature, based on tests of real vehicles on standardized cycles and [26]. While our value for efficiency is higher, it is in alignment with these other sources, because of differences in definition.

A laboratory test of a 2012 Nissan Leaf over the UDDS City cycle found efficiency values of of 118% at 72 °F and ~60% for a 20 °F [15]. Unfortunately, our method needs a cycle-averaged value of powertrain efficiency, so these values cannot be directly used in our model without some way to adjust them to different drive cycles.

Another question to address with our definition powertrain efficiency is how it varies with changes in drive cycle. While our definition of powertrain efficiency is a cycle-averaged value and should yield accurate estimates of battery energy in aggregate, the size of the variation should be investigated. A few studies have addressed this issue, but only for hybrid electric vehicles [111, 11]. Unfortunately, there were no previous studies of powertrain efficiency for electric-only powertrains, and it is inappropriate to extrapolate from hybrid powertrains to electric-only ones, leaving no data to compare these results with. An alternative method would be to adopt the method proposed by Ott et. al, which uses a formulation of powertrain efficiency that separates propulsion and regenerative braking efficiencies, which are claimed to be more consistent across drive cycles [72].

4.2.4 Validation of battery energy comparisons

The method presented above uses one value to represent usable energy of a battery. The usable energy remains relatively constant in the range of battery discharge power

[10] `http://www.teslamotors.com/goelectric/efficiency`

experienced in driving, so not much accuracy is lost by using only one value to refer to usable energy under different conditions. This section further defines the quantity that is measured, and supports the definition with reasoning and evidence.

In this research, any comparison of battery energy across different discharge scenarios must be made carefully to ensure that the comparison is meaningful. Since the usable energy extracted from a battery varies with how it is used, it is hard to compare. For example, a high-power trip that has a calculated required battery energy of 10 kWh actually has slightly higher energy requirement than a 10 kWh low-power trip. Namely, that a battery that can provide 10 kWh at low-power may not be able to do so at high power. This power dependency of energy is of concern when tail fractions are calculated, because then the quantities being compared refer to different scenarios.

The comparison is relevant in calculating a tail fraction, which is the fraction of trips whose energy requirement is too high for the battery to meet. Not accounting for the power dependency of energy might cause misclassification of trips and cause error in the estimated tail fraction. For example, imagine a battery with a capacity of 10 kWh when measured in a medium-power setting. Misclassification error may occur if this capacity is compared to trip energy requirements without addressing the change in usable energy under different discharge power – a high-power trip that used 9.5 kWh might belong in the tail fraction, whereas low-power trip that used 10.5 kWh might not.

The method for this validation test is the following. For each GPS trip, tractive power is calculated at each moment in time, which is then converted to battery power by dividing by powertrain efficiency. Power is divided by the Nissan Leaf's battery mass to find specific power of the battery system. For each GPS trip, the 85th, 90th, 95th, 99th, and 100th percentiles of the trip's list of positive values of specific power are calculated. Then, the distribution of each of these percentiles can be plotted as a histogram and a cumulative density function, shown in Figure 4-4. For example, the bolded line represents the distribution of the 99th percentile of specific power of each trip, across all GPS trips.

Moving forward, technology performance will be compared to the specific power requirements of trips. To do this, a benchmark is selected to represent specific power demand of trips: the 99th percentile of the distribution of 99th percentiles of all trips, the value of which is shown as the vertical black line in the lower panel of Figure 4-4. A battery that can meet this level of performance would be able to reasonably drive over 99% of all trips, having insufficient power for only 1% of the time in these trips.

With this benchmark to represent the maximum battery power required for real-world driving, the performance of technology is compared using the Ragone plot in Figure 4-5. The benchmark appears again as a vertical line. The Ragone plot shows the performance of typical battery chemistries, using system-level metrics. The data for the Ragone plot was taken from [85]. As in the ARPA-E targets [7], battery systems are assumed to have twice the mass of battery cells, so the data is multiplied by 0.5 to convert from cell-level to system-level metrics. The USABC and ARPA-E targets for usable specific energy are plotted here as well.

Figure 4-5 shows that the power requirement of real-world driving is below the

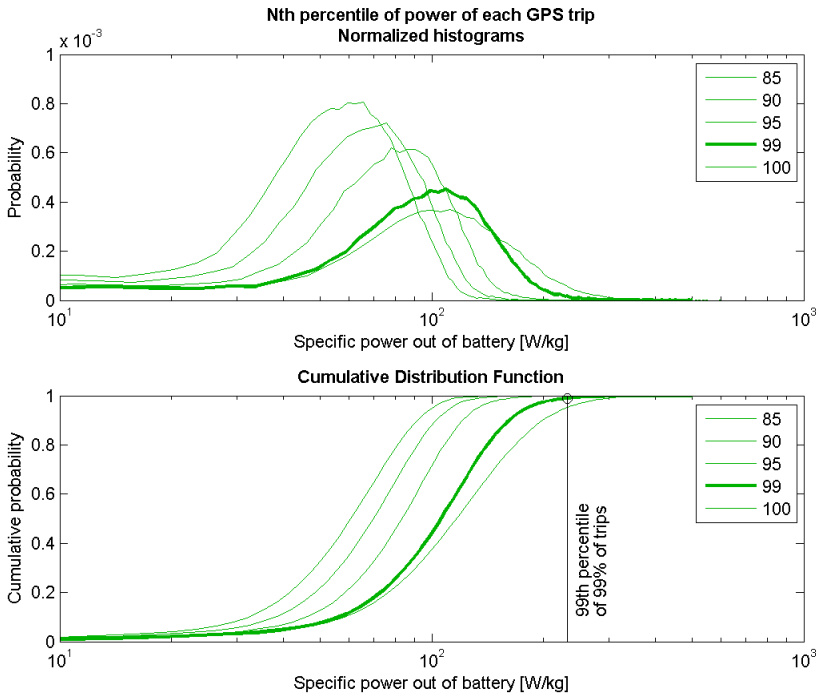

Figure 4-4: Histogram (upper) and cumulative distribution function of battery specific power requirements for real-world GPS drive cycles. A single curve represents the Nth percentile of instantaneous specific power of a trip, across all GPS trips.

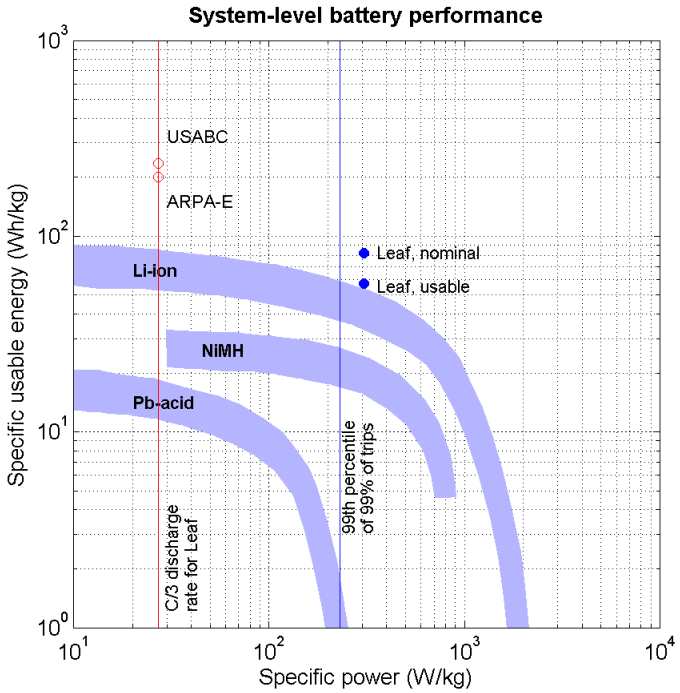

Figure 4-5: Ragone plot of battery performance, using system-level metrics. The vertical black line is a benchmark that represents the maximum battery power required for real-world driving. The red line corresponds to the C/3 discharge rate for the 2011 Nissan Leaf battery, calculated based on the Leaf's nominal battery energy.

"shoulder" of the Ragone curve. Thus, the power requirements of real-world driving stays in the regime where energy does not vary drastically with power, for Li-ion batteries. The Ragone plot also shows the size of the expected variation. At very low power of 10 W/kg, the maximum usable specific energy of Li-ion is 90 Wh/kg. At the maximum power requirement for real-world driving, the usable specific energy is 60 W/kg. In the medium power range of the C/3 discharge rate specified in the USABC and ARPA-E targets, the usable specific energy is 80 Wh/kg. This represents an upper bound on the difference in energy measured in different conditions, because real-world drive cycles experience a variety of power discharge rates, and so would tend to converge towards the mean. Therefore, the difference is small enough for this effect to be ignored when different values of energy are compared.

4.3 Combining datasets across scales

This section explains how the model is applied to estimate battery energy requirements for NHTS trips. This involves two steps: correcting for rounding error and performing a conditional bootstrap procedure to merge the two datasets. The following Figure 4-6 provides an overview of this process.

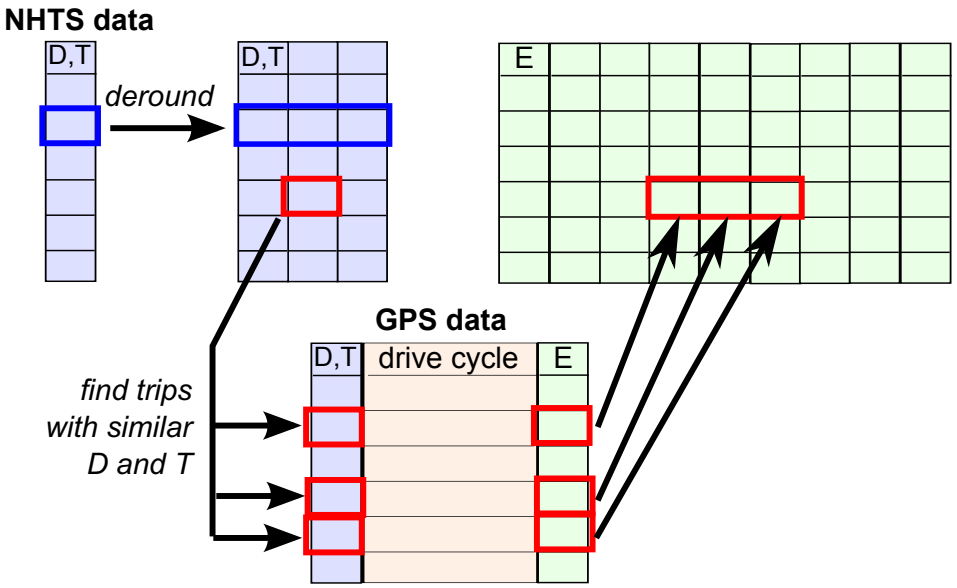

Figure 4-6: Overview of the procedure for combining datasets, which takes NHTS trips as input, and outputs a set of possible tractive energy for each input trip. First, a raw NHTS trip distance and duration are de-rounded into several values (blue boxes). Next, the conditional bootstrap occurs (red boxes), which for a given pair of D and T, finds a set of GPS trips with similar D and T, and returns the corresponding tractive energy for each D and T.

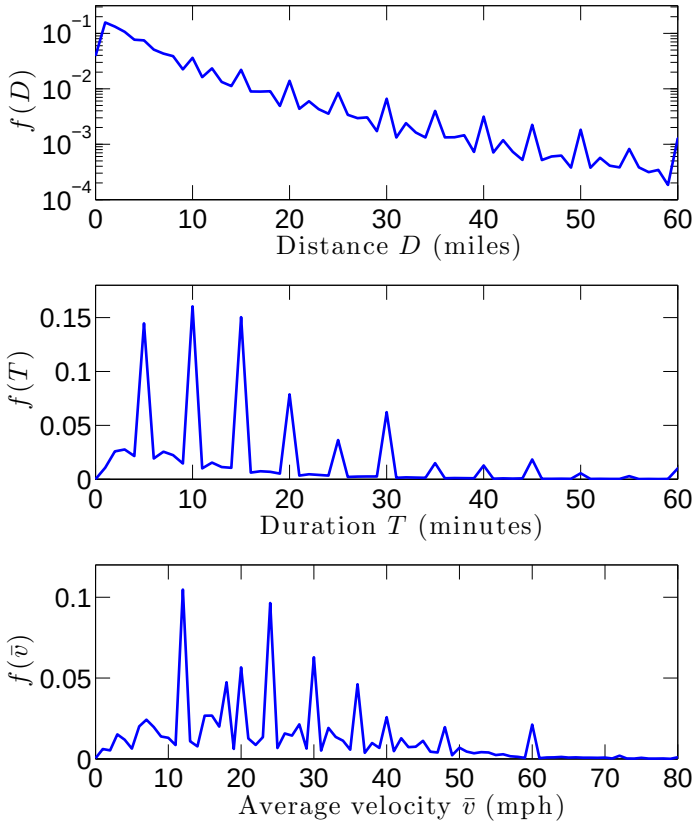

Figure 4-7: Distributions of raw values of NHTS vehicle trip distance, duration, and average velocity. The peaks are evidence of the tendency of survey subjects to round their responses to the nearest multiple of 5 or 15.

4.3.1 Correcting for rounding error in NHTS data

A first step in preparing the raw NHTS data for analysis is to correct for rounding error in the distance and duration records through a process called "de-rounding". The NHTS data is self-reported by the survey subjects, who seem to have a tendency to round their responses to the nearest 5 or 15 for convenience when reporting trip distances or durations. This is evidenced by unnatural peaks in the distribution of distance and duration values, as shown in Figure 4-7. While such rounding error in the data would not affect certain statistical measures such as the mean, analyses based on the distribution of the data can be biased [28]. The goal is to redistribute the data in the peaks to nearby values in a way that creates a more realistic distribution, without introducing bias to the data.

The approach used is to convert the raw NHTS values to "true" values, which will try to mimic the distribution of distance and duration prior to rounding. Each raw data point will be mapped to a handful of possible "origin" points, representing the potential true values that, when rounded, could yield the observed value. This is the first step shown in Figure 4-6. The following section explains the mathematical

details of this process, in which a model of rounding is first developed, and then statistics is applied to select possible origin values. This section is based on the de-rounding method developed for an upcoming paper [61].

Let x denote the true value of some quantity, and $\tilde{x}$ the corresponding rounded value that is observed. The set of observed data provides the probability mass function of $\tilde{x}$, $P(\tilde{x})$. The goal is to estimate the probability density of x, $p(x)$, which can be computed from $P(\tilde{x})$ with

$$p(x) = \sum_{\tilde{x}} p(x|\tilde{x})\, P(\tilde{x}), \tag{4.2}$$

where $p(x|\tilde{x})$ is the conditional probability that the true value was x, given that the value observed was $\tilde{x}$. This conditional probability $p(x|\tilde{x})$ needs to be computed.

First, a probabilistic model of the rounding process is devised as follows. For a given true value x, it is rounded to the nearest multiple of 1 (i.e. integer) with probability P_1, the nearest multiple of 5 with probability P_5, and nearest multiple of 15 with probability P_{15}. Since one of the rounding options must occur, $P_1+P_5+P_{15} = 1$. These probabilities will be referred to the "rounding probabilities". Multiples of 1, 5, and 15 are chosen as the rounding rules because they best describe the NHTS data: 1 is chosen because the data values are integers, and 5 and 15 are chosen because they are the locations of the unusually large peaks. For conciseness, let $R_k(x)$ mean "x rounded to the nearest the nearest multiple of k"; e.g. $R_5(23) = 25$ and $R_{15}(23) = 30$. Then the probability of rounding from x to $\tilde{x}$ is

$$P(\tilde{x}|x) = \begin{cases} P_1 & \tilde{x} = R_1(x) \\ P_5 & \tilde{x} = R_1(x) \\ P_{15} & \tilde{x} = R_{15}(x) \\ 0 & \text{otherwise} \end{cases}.$$

The reverse probability $p(x|\tilde{x})$ is needed to find $p(x)$ in Equation 4.2. To express this term, the three cases of rounding in the observed data will be considered separately: (1) $\tilde{x}$ is a multiple of 1 only, (2) $\tilde{x}$ is a multiple of 1 and 5, and (3) $\tilde{x}$ is a multiple of 1, 5, and 15.

If the observed value $\tilde{x}$ is only a multiple of 1, then the original value x must have been "1-rounded", i.e. rounded to the nearest multiple of 1. Therefore, x must have originated in the interval $\left[\tilde{x} - \frac{1}{2}, \tilde{x} + \frac{1}{2}\right]$. For simplicity, x is assumed to be uniformly distributed in this interval, so the reverse probability is

$$p(x|\tilde{x}) = \begin{cases} 1 & x \in \left[\tilde{x} - \frac{1}{2}, \tilde{x} + \frac{1}{2}\right] \\ 0 & \text{otherwise} \end{cases}.$$

If $\tilde{x}$ is a multiple of 1 and 5, then the original value x must have been either "1-rounded" or "5-rounded", and x could be anywhere in $\left[\tilde{x} - \frac{5}{2}, \tilde{x} + \frac{5}{2}\right]$. If x is again assumed to be uniformly distributed in this interval, then $p(x|\tilde{x})$ will resemble a

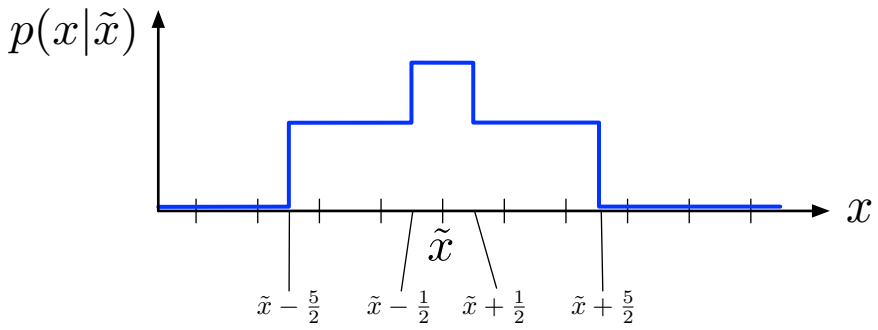

Figure 4-8: "Staircase" shaped conditional distribution of $p(x|\tilde{x})$ when $\tilde{x}$ is a multiple of 5.

staircase shape, as shown in Figure 4-8. This staircase shape exists because the probability of x being in the outer intervals of $\left[\tilde{x}-\frac{5}{2},\tilde{x}-\frac{1}{2}\right]$ and $\left[\tilde{x}+\frac{1}{2},\tilde{x}+\frac{5}{2}\right]$ is proportional to P_5, because it must have been 5-rounded, whereas the probability of x being in the inner interval of $\left[\tilde{x}-\frac{1}{2},\tilde{x}+\frac{1}{2}\right]$ is proportional to P_1+P_5, because it could have been either 1-rounded or 5-rounded. Normalizing this distribution yields:

$$p(x|\tilde{x}) = \begin{cases} P_5/A & x \in \left[\tilde{x}-\frac{5}{2},\tilde{x}-\frac{1}{2}\right] \\ (P_1+P_5)/A & x \in \left[\tilde{x}-\frac{1}{2},\tilde{x}+\frac{1}{2}\right] \\ P_5/A & x \in \left[\tilde{x}+\frac{1}{2},\tilde{x}+\frac{5}{2}\right] \\ 0 & \text{otherwise} \end{cases}$$

where

$$A = P_1 + 5P_5.$$

If $\tilde{x}$ is a multiple of 1, 5, and 15, the distribution is a 3-level staircase, with 5 regions accounting for the 3 different ways of rounding to $\tilde{x}$, following the same logic as above. The result is:

$$p(x|\tilde{x}) = \begin{cases} P_{15}/B & x \in \left[\tilde{x}-\frac{15}{2},\tilde{x}-\frac{5}{2}\right] \\ (P_5+P_{15})/B & x \in \left[\tilde{x}-\frac{5}{2},\tilde{x}-\frac{1}{2}\right] \\ (P_1+P_5+P_{15})/B & x \in \left[\tilde{x}-\frac{1}{2},\tilde{x}+\frac{1}{2}\right] \\ (P_5+P_{15})/B & x \in \left[\tilde{x}+\frac{1}{2},\tilde{x}+\frac{5}{2}\right] \\ P_{15}/B & x \in \left[\tilde{x}+\frac{5}{2},\tilde{x}+\frac{15}{2}\right] \\ 0 & \text{otherwise} \end{cases}$$

where

$$B = P_1 + 5P_5 + 15P_{15}.$$

Now, a method is needed to estimate the values for P_1, P_5, and P_{15} based on the data. First, the expected size of the peaks in the rounded data, based on the rounding model, is considered. Given the true distribution $p(x)$, the model predicts that the observed distribution $\tilde{P}(\tilde{x})$ will be

$$\tilde{P}(\tilde{x}) = P_1 \int_{\tilde{x}-\frac{1}{2}}^{\tilde{x}+\frac{1}{2}} p(x)\, dx$$

when $\tilde{x}$ is a multiple of only 1, and

$$\tilde{P}(\tilde{x}) = P_1 \int_{\tilde{x}-\frac{1}{2}}^{\tilde{x}+\frac{1}{2}} p(x)\, dx + P_5 \int_{\tilde{x}-\frac{5}{2}}^{\tilde{x}+\frac{5}{2}} p(x)\, dx$$

when $\tilde{x}$ is a multiple of only 1 and 5, and

$$\tilde{P}(\tilde{x}) = P_1 \int_{\tilde{x}-\frac{1}{2}}^{\tilde{x}+\frac{1}{2}} p(x)\, dx + P_5 \int_{\tilde{x}-\frac{5}{2}}^{\tilde{x}+\frac{5}{2}} p(x)\, dx + P_{15} \int_{\tilde{x}-\frac{15}{2}}^{\tilde{x}+\frac{15}{2}} p(x)\, dx$$

when $\tilde{x}$ is a multiple of 1, 5, and 15. To simply these integrals, $p(x)$ is approximated as uniformly distributed near $\tilde{x}$, yielding the following equations:

$$\begin{aligned} \tilde{P}(\tilde{x}) &= P_1 \\ \tilde{P}(\tilde{x}) &= P_1 + 5P_5 \\ \tilde{P}(\tilde{x}) &= P_1 + 5P_5 + 15P_{15}. \end{aligned} \tag{4.3}$$

Now, consider three consecutive bins in the observed distribution, $\tilde{x}-1$, $\tilde{x}$, and $\tilde{x}+1$, where the middle bin is a multiple of only 1 and 5. The data enables measurement of the ratio

$$\rho_5 \equiv \frac{\tilde{P}(\tilde{x})}{\left[\tilde{P}(\tilde{x}-1) + \tilde{P}(\tilde{x}+1)\right]/2}, \qquad \tilde{x} \text{ is multiple of 1 and 5,}$$

which describes how much higher the peak bin is than the average level of its two neighbors. Using Equation 4.3, the ratio is approximately

$$\rho_5 \approx 1 + 5\frac{P_5}{P_1}.$$

A similar ratio can be defined for bins that are multiples of 1, 5, and 15:

$$\rho_{15} \equiv \frac{\tilde{P}(\tilde{x})}{\left[\tilde{P}(\tilde{x}-1)+\tilde{P}(\tilde{x}+1)\right]/2}, \qquad \tilde{x} \text{ is multiple of 1, 5, and 15}$$

which the model predicts to be approximately

$$\begin{aligned}\rho_{15} &\approx 1 + 5\frac{P_5}{P_1} + 15\frac{P_{15}}{P_1} \\ &= \rho_5 + 15\frac{P_{15}}{P_1}.\end{aligned}$$

By calculating these two ratios, combined with the constraint that $P_1+P_5+P_{15} = 1$, a solution for the three rounding probabilities can be found. Some algebra yields these results:

$$\begin{aligned}P_1 &= \frac{1}{1+\frac{1}{5}(\rho_5-1)+\frac{1}{15}(\rho_{15}-\rho_5)} \\ P_5 &= \frac{1}{5}(\rho_5-1)P_1 \\ P_{15} &= \frac{1}{15}(\rho_{15}-\rho_5)P_1.\end{aligned} \tag{4.4}$$

In the above derivation, only the two neighboring bins are used to calculate the ratios in order to minimize the bias caused by deviations from non-uniformity in $p(x)$. Since the bins are close together, the true distribution is expected to be similar for each bin, and therefore the observed difference between the bins would come from the tendency of true values to be rounded into the middle peak bin. Differences between the peak bin and bins further away are caused by both rounding and true differences in $p(x)$. An alternative option would be to compute ratios from additional bins, such as the 4 nearest bins, rather than just the nearest 2. This would increase the bias from deviations from the assumption of uniform $p(x)$ near $\tilde{x}$, but it would also decrease the method's sensitivity to noise in the data.

In practice, the ratios ρ_5 and ρ_{15} used in Equation 4.4 are computed from an aggregation of all the peaks in the data, rather than from any single peak. For example, ρ_5 is computed from sums of the bins adjacent to any multiple of 5, i.e. the sum of any bin corresponding to $\tilde{x}-1$, $\tilde{x}$, or $\tilde{x}+1$. The ratio is then computed from these three aggregated bins. The same procedure is applied to peaks at multiples of 15. The following equations summarizes this procedure:

$$\tilde{P}_{agg,5}(\tilde{x}-1) = \sum_{\tilde{x} \text{ is multiple of } 5} \tilde{P}(\tilde{x}-1)$$
$$\tilde{P}_{agg,5}(\tilde{x}) = \sum_{\tilde{x} \text{ is multiple of } 5} \tilde{P}(\tilde{x})$$
$$\tilde{P}_{agg,5}(\tilde{x}+1) = \sum_{\tilde{x} \text{ is multiple of } 5} \tilde{P}(\tilde{x}+1)$$
$$\rho_5 \equiv \frac{\tilde{P}_{agg,5}(\tilde{x})}{\left[\tilde{P}_{agg,5}(\tilde{x}-1) + \tilde{P}_{agg,5}(\tilde{x}+1)\right]/2},$$

$$\tilde{P}_{agg,15}(\tilde{x}-1) = \sum_{\tilde{x} \text{ is multiple of } 15} \tilde{P}(\tilde{x}-1)$$
$$\tilde{P}_{agg,15}(\tilde{x}) = \sum_{\tilde{x} \text{ is multiple of } 15} \tilde{P}(\tilde{x})$$
$$\tilde{P}_{agg,15}(\tilde{x}+1) = \sum_{\tilde{x} \text{ is multiple of } 15} \tilde{P}(\tilde{x}+1)$$
$$\rho_{15} \equiv \frac{\tilde{P}_{agg,15}(\tilde{x})}{\left[\tilde{P}_{agg,15}(\tilde{x}-1) + \tilde{P}_{agg,15}(\tilde{x}+1)\right]/2},$$

Each observed value is assigned a handful of true values by randomly sampling from the reverse distribution function determined by P_1, P_5, and P_{15}. In the practical implementation of this method, 4 true values are assigned for each observed value. Multiple values for each observed value are assigned to reduce the bias introduced by the random generation process. The survey weights in the NHTS data are adjusted to account for the replication of data points.

More sophisticated de-rounding methods could be devised, though for simplicity the above procedure is used. For example, the rounding model could be made more elaborate by including more ways to round (e.g. a P_{10}), or by using a different kernel to represent the "likelihood to round" rather than uniform. A possible improvement to solving for $p(x)$ would be to make it iterative. The estimated $p(x)$ distribution from the first iteration could be used in place of the uniformity assumption in the second iteration, and so forth.

4.3.2 Conditional bootstrap procedure

This section explains the method used to assign tractive energy requirements to NHTS trips based on the GPS data. This method is based on the one used by McNerney et al. in an upcoming paper [61], which in turn is based on the method from [23].

The goal is to estimate the distribution of tractive energy requirements from the NHTS data, but these trips only have records of distance and duration, which are not enough to estimate tractive energy as accurately as this research requires. The GPS data has drive cycle data which does allow accurate estimation of tractive energy,

but doesn't have the broad regional and segmental scope of the NHTS. To address these data issues, a conditional bootstrap procedure is used to compute the energy distribution associated with the NHTS data by inputting energies from the GPS data, thereby combining broad regional scope with accurate estimation of energy.

The overall structure of this procedure is to, for every observed trip in the NHTS, identify a set of "similar" GPS trips, based on distance and duration, and then assign the tractive energy requirements from the set of similar GPS trips to the original NHTS trip. This bootstrap procedure is the second step of Figure 4-6, highlighted in red. This section presents the mathematical details of this conditional bootstrap procedure.

The first step is to re-write the expression for energy into another form that can help bridge the two datasets. The following identity is used:

$$E = (\frac{E}{D})D.$$

The energy intensity of a trip is denoted by F. The letter F (not to be confused with force) is used because energy intensity is related to fuel consumption. Note that this is the same quantity as the energy-per-mile EPM quantity used in the powertrain derivation, but F is used here for brevity. Energy intensity of a trip is defined as the tractive energy requirement of a trip, divided by its distance:

$$F \equiv E/D$$

which gives us

$$E = FD.$$

This expression is useful because it separates the quantities known in the NHTS data, namely distance D, from those quantities that require knowledge of the drive cycle to be calculated effectively, namely energy intensity F. The approach that will be used is to compute F for each GPS trip, and use that information to augment the NHTS data using the conditional bootstrap procedure.

Next, the law of total probability allows the probability density of $p(E)$ of trip tractive energies E to be written as

$$p(E) = \iiint p\big(E|D,T,F\big)\, p\big(D,T,F\big)\; dD\; dT\; dF. \tag{4.5}$$

This equation states that the probability of a random NHTS trip having energy E is equal to the probability of a trip having a particular combination of (D,T,F) times the probability that this combination yields energy E, summed over all possible combinations of (D,T,F).

Equation 4.5 can be worked into a more convenient form that will motivate the conditional bootstrap procedure. Since D and F alone are sufficient to specify the

energy E, the conditional probability $p(E|D,T,F)$ is a delta function:

$$\begin{aligned} p\big(E\big|D,T,F\big) &= \delta\Big(E - E(D,T,F)\Big) \\ &= \delta(E - FD). \end{aligned} \tag{4.6}$$

Using the definition of conditional probability, $p(D,T,F)$ can be split into two parts:

$$p\big(D,T,F\big) = p\big(F\big|D,T\big)\, p\big(D,T\big). \tag{4.7}$$

Equation 4.7 shows that the probability of observing a (D,T,F) triplet is equal to the probability of observing a (D,T) pair times the probability of observing F given the observed (D,T) pair. This decomposition is useful because $p(D,T)$ is known from the NHTS dataset, because there is a probability mass $1/N$ associated with each of the N observations (D_i,T_i). Therefore,

$$p\big(D,T\big) = \sum_{i=1}^{N} \frac{1}{N} \delta(D - D_i)\delta(T - T_i). \tag{4.8}$$

Plugging in Equation 4.6, Equation 4.7, and Equation 4.8 into Equation 4.5 yields

$$p(E) = \frac{1}{N} \sum_{i=1}^{N} \int \delta\Big(E - FD_i\Big)\, p\big(F\big|D_i,T_i\big)\; dF. \tag{4.9}$$

This is a sum over all N (D_i,T_i) pairs in the NHTS data. For each term of the sum, there is an integral of the probability that a trip with the observed (D_i,T_i) has a value of F such that $E = FD_i$. Note that for a specified value of D_i, there is only one value of F that yields energy E.

Trip duration T is included in the above derivation because T provides additional information in estimating the conditional probability $p(F|D,T)$, thus improving the accuracy of the estimation. An alternative would be to use $p(F|D)$, since energy can be determined by only D and F. This has the advantage of lower dimensionality, which leads to a higher density of points to sample from in the conditional bootstrap at the cost of higher bias due to ignoring the dependence of F on T.

Equation 4.9 can be read as a prescription for the following conditional bootstrap procedure: for each trip in the NHTS, grab its distance and duration as the pair (D_i,T_i); generate plausible values for energy intensity F given (D_i,T_i); compute the resulting energy $E = FD_i$; and add it to a list. Repeat this many times for each trip, then repeat for all trips, and then compute the distribution of the whole list. This procedure will create a distribution of F that resembles the true distribution of $p(F|D_i,T_i)$, if plausible F are generated properly.

The method for generating plausible F is based on the approach in [23]. The estimated conditional density $\hat{p}_h(F|D_i,T_i)$ is written as

$$\hat{p}_h\big(F\big|D,T\big) = \sum_{g=1}^{G}\left[\frac{K\left(\frac{\Delta-\Delta^{(g)}}{h}\right)}{\sum_{r=1}^{G}K\left(\frac{\Delta-\Delta^{(r)}}{h}\right)}\cdot\frac{K\left(\frac{\Theta-\Theta^{(g)}}{h}\right)}{\sum_{s=1}^{G}K\left(\frac{\Theta-\Theta^{(s)}}{h}\right)}\right]\delta(F-F^{(g)}), \quad (4.10)$$

where K is a kernel function, h is the bandwidth, $\Delta \equiv \log_{10} D$, and $\Theta \equiv \log_{10} T$. The sums run over all G trips in the GPS dataset. D and T are distances and durations passed in from the NHTS dataset, while $D^{(g)}$ and $T^{(g)}$ are distances and durations from trip g from the GPS dataset. $K(x)$ is a kernel function that controls the likelihood of selecting of a particular $(D^{(g)}, T^{(g)})$ based on its distance to (D, T); if a given $(D^{(g)}, T^{(g)})$ is close to (D, T), it will have a high probability of selection. The bandwidth h tunes the necessary distance between the pairs. Distance between points is defined logarithmically because trip distances and durations are spread out over several orders of magnitude.

For simplicity, the uniform kernel is used: $K(x) = 1$ if $x \in [-1, 1]$ and $K(x) = 0$ otherwise. This choice of kernel stipulates that all $F^{(g)}$ whose corresponding $\Delta^{(g)}$ and $\Theta^{(g)}$ are each within distance h to Δ and Θ, respectively, are equally likely to be selected. This choice of kernel lends itself nicely to a bootstrap simulation by simplifying the sampling procedure: rather than taking the sum in the denominators over all GPS trips, a handful of trips is randomly selected from the rectangular sampling space defined by the kernel and bandwidth.

In practice, the sparsity of data at higher values of D and T means that sometimes there may not be any GPS trips in the default sampling window. To solve this, the sampling window is gradually expanded by increasing h until it bounds a satisfactory amount of trips, from an initial value of $h = 0.125$.

In summary, the steps of the algorithm are listed below:

1. Take a trip i from the NHTS data and get its distance D_i and duration T_i.

2. Find the set S_i of "similar" GPS trips, whose distances and durations are each within log-distance h of (D_i, T_i).

3. In each bootstrap world b, select a GPS trip g uniformly from S_i, and assign the bootstrapped energy intensity $F^{(ib)} = F^{(g)}$.

4. Calculate the bootstrapped tractive energy requirement $E_{ib} = F^{(ib)} D_i$, and record it to a list.

5. Repeat steps 1-4 many times, to generate many bootstrap worlds to obtain a large selection of possible $F^{(ib)}$ that could have occurred with the NHTS trip i.

6. Repeat steps 1-5 for each trip i in the NHTS data.

7. Compute the empirical density of the list $\{E_{ib}\}$.

In the implementation of this method, 4 possible values are chosen for $F^{(ib)}$ for each NHTS trip i in step 4.

There are alternative methods for selecting F based on (D, T) other than this conditional bootstrap. Other studies have used a single constant value for F, which were mentioned in Section 2.4. F could also be calculated from a regression on both D and T. However, a conditional bootstrap procedure is preferred because it preserves the natural variation in F observed in the GPS data, which creates a more representative distribution of tractive energy.

4.3.3 Validation of conditional bootstrap procedure

This section validates the conditional bootstrap density estimation procedure by assessing the accuracy of its predictions of trip energy on the GPS dataset. For each trip, the bootstrapped energy is compared with the "true" energy, which is calculated directly from the drive cycle. If the method works, the bootstrap output should, on average, match up with the true energy values. While accuracy for individual trips would be ideal, it is more important to see whether the using the bootstrap method introduces bias in the main metric of interest in this analysis: tail fraction (fraction of energy above a certain threshold).

The details of the validation are as follows. First, the GPS dataset is split into a 1000-trip test set and a 64,632-trip reference set. The test set is modified to mimic NHTS data by simulating the rounding of the trip distances and durations. The test set is then fed through the model: first, the distances and durations are de-rounded into 4 distance-duration pairs. Next, each of the de-rounded distance-duration pairs are matched with 4 similar trips from the reference set, thus assigning 16 total possible energy values to each of the 1000 trips in the test set. This constitutes one run of the bootstrap simulation. A total of 100 bootstrap simulations are run with different partitions of the GPS data, in order to study the difference in error metrics with respect to different partitions of the GPS data.

In the analysis below, "per-trip error" is defined as the difference between the mean of the 16 bootstrapped energies and the true energy value, which is calculated from the drive cycle of the trip. Information for properly aggregating vehicle-trips into vehicle-days was not readily available in the GPS dataset, so vehicle-days were simulated by first choosing the number of trips per day by sampling from a Poisson distribution with mean 3.5, then assigning the 1000 test trips randomly to vehicle-days. Energies for vehicle-days were calculated by summing up the means of the energies of the constituent trips. The threshold used for calculation of tail fractions is the 16.8 kWh usable energy of the Leaf battery, which is assumed to be 70% of its 24 kWh nominal energy capacity[11].

Figure 4-9 shows both absolute prediction error (panel 1) and relative prediction error (panel 2) for each trip in the test set, for one bootstrap simulation. Prediction error is the difference between the predicted energy and the true value. The mean error is slightly negative. The scatterplot shows that the variance in prediction error scales up with higher predicted trip energies, as expected. In the second panel, a linear fit of the errors indicates that energies of high-energy trips might be overestimated while low-energy trips are underestimated.

Figure 4-9 shows the results for one bootstrap run, but it is important to see

[11] See Subsection 5.3.3 for a detailed explanation of "usable energy" used in this way.

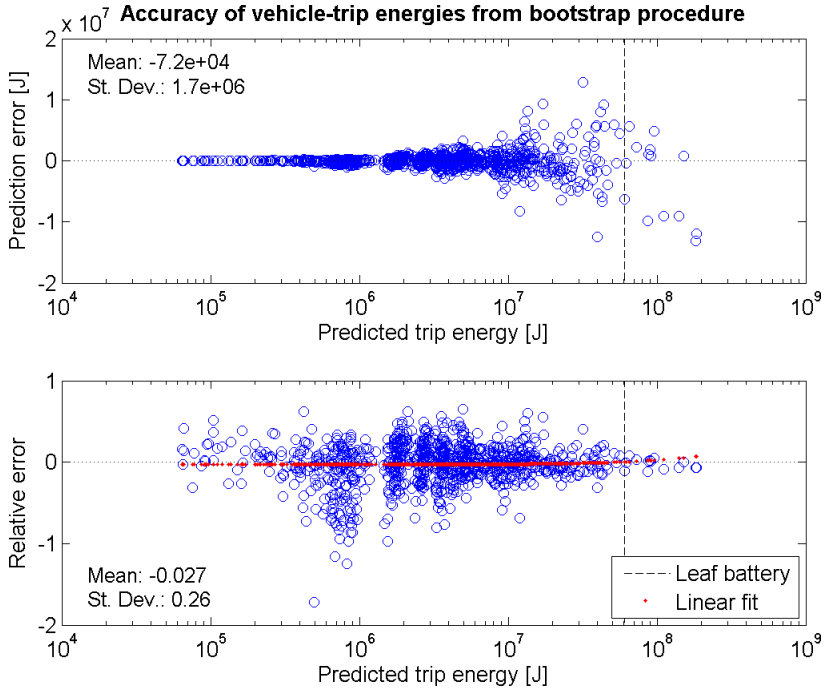

Figure 4-9: Accuracy of vehicle-trip energies estimated with the conditional bootstrap procedure. Absolute per-trip prediction error (top) and relative per-trip prediction error are plotted against predicted energy, for a single bootstrap simulation. A linear fit (in red) is shown for percent error, which indicates overestimation of energy for high-energy trips.

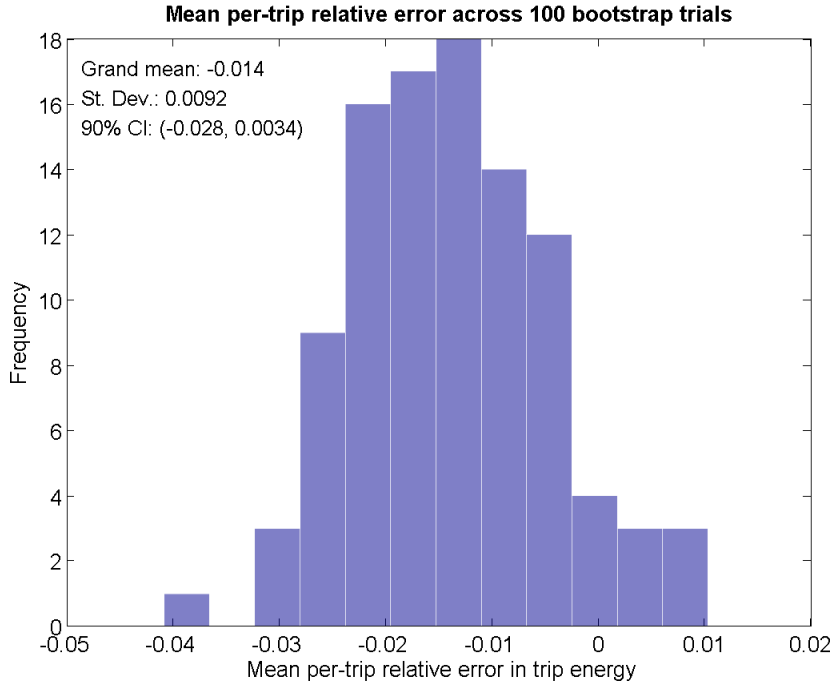

Figure 4-10: Histogram of mean per-trip relative prediction error in trip energies.

whether these trends persist over repeated runs of the bootstrap procedure, i.e. with different mappings of survey trips to GPS trips and with different partitions of the GPS data into test and reference sets. To see how the mean of the per-trip relative error changes, this metric is compared across bootstrap trials. From the list of mean per-trip relative error from each of the 100 bootstrap trials, a grand mean and the standard error are calculated. The distribution of the means and the summary statistics are shown in Figure 4-10. Treating the mean error from each bootstrap trial as a random variable, a 90% confidence interval for the grand mean is calculated by using the observed 5th and 95th percentiles as the boundaries of the interval. This confidence interval contains 0, which means that the results do not reject the null hypothesis that the true mean is 0. While the grand mean is slightly negative, the test does not show it is statistically significantly different from 0.

Therefore, this analysis shows that the method is accurate enough in estimating the energies of individual trips. While there may be some slight negative bias, it is not statistically significant, and is much smaller than other potential sources of error in the model.

In addition to the overall model behavior described by the grand mean of prediction error, the error in predictions of tail fractions is also of interest, because some of the results and conclusions in this thesis depend on the model's estimates of tail fraction. Errors in tail fraction estimates occur when trips are misclassified as being counted in or out of the tail fraction, because the estimated energy and actual energy of a trip are on different sides of the tail fraction threshold. For example, the model's estimate of energy for a trip could be above threshold, counting it as part

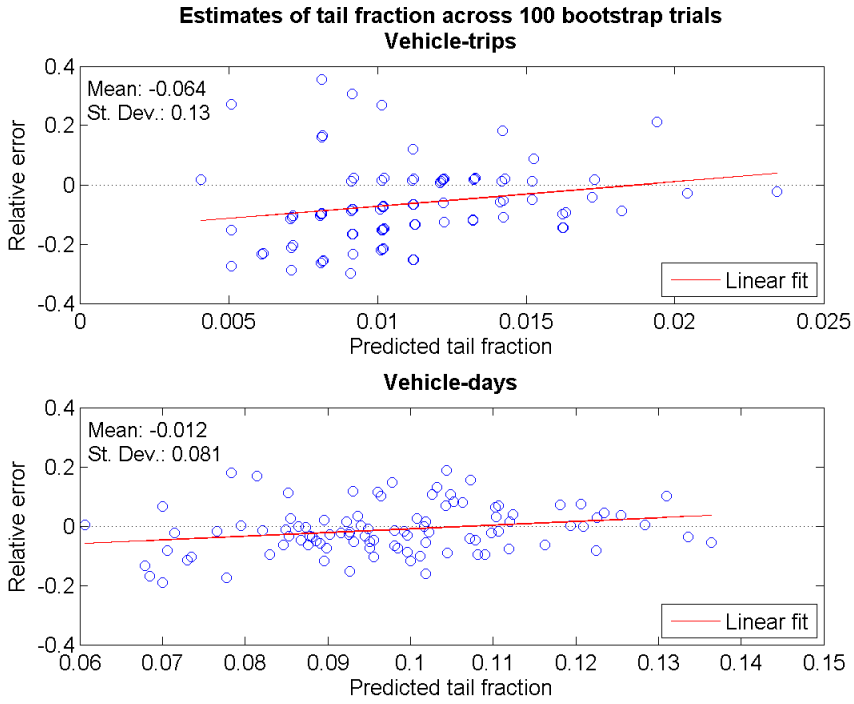

Figure 4-11: Scatterplot of relative error in tail fraction versus predicted tail fraction.

of the tail fraction, while in reality its energy is below the threshold.

Figure 4-11 shows the relative error in the predicted tail fraction versus the predicted tail fraction. First, it is noted that the tail fraction varies over a wide range, from 0.005 to 0.025 for vehicle-trips and 0.06 to 014 for vehicle-days. The size of the variation is impacted by the sample size of the test set, so increasing it above 1000 trips may reduce this observed variation. However, a sample size of 1000 trips is used to simulate running the model on a small number of trips, on the order of the number of NHTS trip records for a small US city. The results show that the error in tail fraction has a negative mean, and that the linear fit indicates a smaller amount of relative error for larger predicted tail fractions. To further understand the origin of the negative bias, prediction error for trips near the tail fraction are investigated to see whether the method tends to over- or under-estimate energy for these trips. Finally, the graphs show that the absolute error for vehicle-days is about 5 times bigger than that of vehicle-trips, because vehicle-day tail fractions are about 10 times bigger than vehicle-trips, while the standard deviation in the relative error for vehicle-trips is only twice that of vehicle-days.

Figure 4-12 focuses on the relative errors by discarding the X-axis from Figure 4-11 and presenting the relative errors in a histogram. The distribution of relative error is wider for vehicle-trips than for vehicle-days, possibly because smaller absolute values of tail fractions for vehicle-days leads to larger relative error for the same absolute error.

While the means of both distributions are negative, the 90% confidence interval in both cases include zero, meaning that the null hypothesis that the bias is 0 cannot

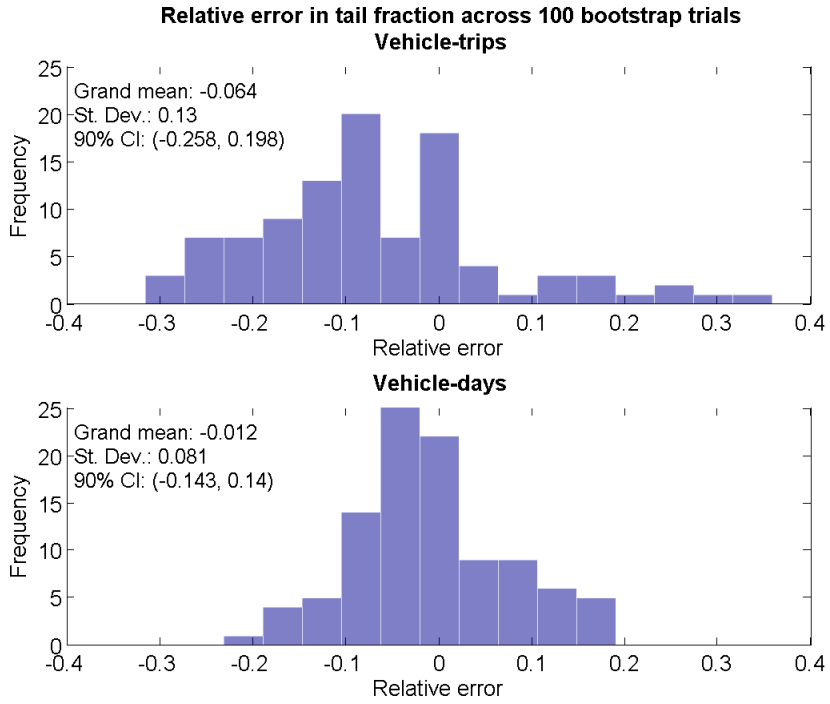

Figure 4-12: Histogram of relative error in tail fraction estimates.

be rejected. However, the histograms show that the variation in relative error is large, ranging up to 20% for vehicle-days. This provides an estimate for the standard error for the tail fraction estimates presented later in the results chapter.

THIS PAGE INTENTIONALLY LEFT BLANK

Chapter 5

Results

This chapter presents the results of the research. In Section 5.1, the travel patterns in the NHTS and GPS datasets are studied without applying the energy model. Section 5.2 shows the results of the energy model and highlights some trends. In Section 5.3, the energy requirements are compared to performance targets for battery energy capacity.

5.1 Characterization of NHTS and GPS trips

Before analyzing the energy requirements of trips, a useful first step is to characterize trip patterns in general, in terms of their distance and duration. This section focuses on studying the raw datasets, before applying the energy model from Chapter 4. First, the relevant units of analysis will be introduced. Next, trip duration, distance, and average velocity will be analyzed for both datasets. Finally, the real-world drive cycles are characterized and described.

5.1.1 Units of analysis

This study uses three units of analysis to classify travel: person-trips, vehicle-trips, and vehicle-days. A person trip is a trip made by an individual person, while a vehicle-trip is a trip made by an individual vehicle. For example, two people going to the airport in the same vehicle counts as two person-trips, but a single vehicle-trip. A vehicle-day is the set of all vehicle-trips occurring on one day for a particular vehicle.

Vehicle-days are the most interesting units of analysis for this thesis, because the energy requirement for a vehicle-day represents the scenario that an EV is driven for a full day, without charging during the day and being charged overnight. This is a better approximation of reality than vehicle-trips, since most PEVs are only charged at home overnight.

Alternative choices for the unit of analysis would place the focus on different aspects of travel. Using person-trips would put the focus on the needs of travelers, but would lead to double-counting of energy requirements for vehicles. Using vehicle-trips would emulate the unlikely scenario that PEVs are recharged after every trip. This could be used as an upper bound for the impact of public charging stations

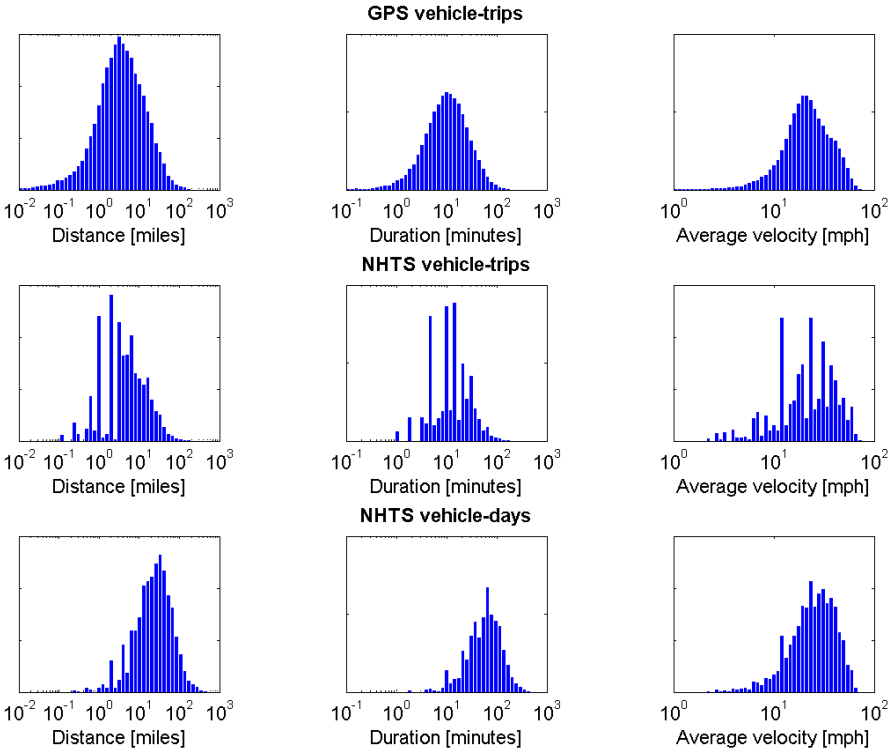

Figure 5-1: Histogram of D, T, and v for GPS vehicle-trips, NHTS vehicle-trips, and NHTS vehicle-days.

on reducing the performance requirement for batteries. In addition, more intelligent combinations of trip chains could better represent real opportunities for charging.

Trips made in personally owned vehicles will be the focus of this thesis, because the goal of this analysis study the potential usage of electric vehicles as personal vehicles. The NHTS contains a variety of trip modes, such as walking, driving, public transportation, etc., which are ignored for this analysis.

5.1.2 Distance, duration, and speed

The analysis begins by looking at the aggregate characteristics of trips - distance (D), duration (T), and average speed (v). Histograms of D, T, and v are shown in Figure 5-1, for GPS vehicle-trips, NHTS vehicle-trips, and NHTS vehicle-days. Note that the histograms are shown on a logarithmic scale, to better represent the full range of these variables. They follow a roughly log-normal distribution, with a small mean but a heavy tail. The large majority of trips occupy a small portion of the entire range, because most of the trips in the dataset are quite short. The 90th, 95th, and 99th percentiles of vehicle-trip distance are 20, 30, and 65 miles, respectively. As a benchmark for distance, the average commute by personal vehicle in the US is 12.09 miles [83]. Finally, the fact that the NHTS and GPS distributions are similar in both center and spread verifies that the GPS trips from California are

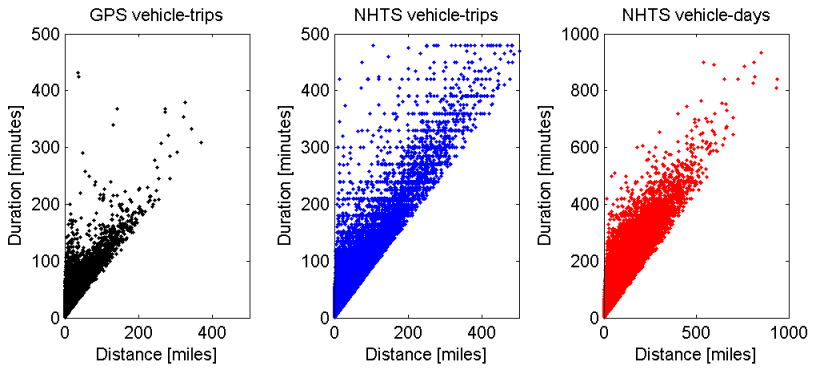

Figure 5-2: Scatterplot of T vs D for GPS vehicle-trips, NHTS vehicle-trips, and NHTS vehicle-days.

reasonably representative of nationwide driving patterns.

To better understand the relationship between distance and duration, scatterplots of the same three units of analysis as above, are shown in Figure 5-2, on axes of T vs D. The first feature to notice about these plots is the triangular shape. There are no points below the lower edge of the triangle because of physical speed limitations. The density of points also decreases at the left-hand edge of triangle, because there are few trips at very low average speeds. Most trips are in a moderate speed range. The second feature is the large density of points near the origin. Most trips have short distance and short duration. This echoes the log-normal shape of the histograms seen in Figure 5-1, with its low mean and heavy tail. Again, the similarity between the GPS scatterplot and the others gives confidence in bootstrapping on the GPS data.

One possible issue is the relative scarcity of GPS data points at long distances and durations. Luckily, this is not a big issue, because the variation in per-mile energy consumption is lower for longer trips, so a smaller number of points is sufficient to represent the variation.

5.1.3 Characterization of drive cycles

The detail offered in the GPS dataset can also be used to characterize how drive cycles change for different aggregate characteristics of trips. To do this, Figure 5-3 shows GPS drive cycles that represent trips from different regions of the D-T space.

This figure gives a physical sense of the types of trips one would expect to find at different ranges. At long distances, trips consist mostly of highway driving, with surface road driving at the start and end. Difference in average trip velocity is mostly explained by different highway cruising speeds, fraction of time spent on surface roads, or the amount of highway traffic. This physical understanding of the types of trips that are represented will also help interpret the energy results from the bootstrap procedure in the next section.

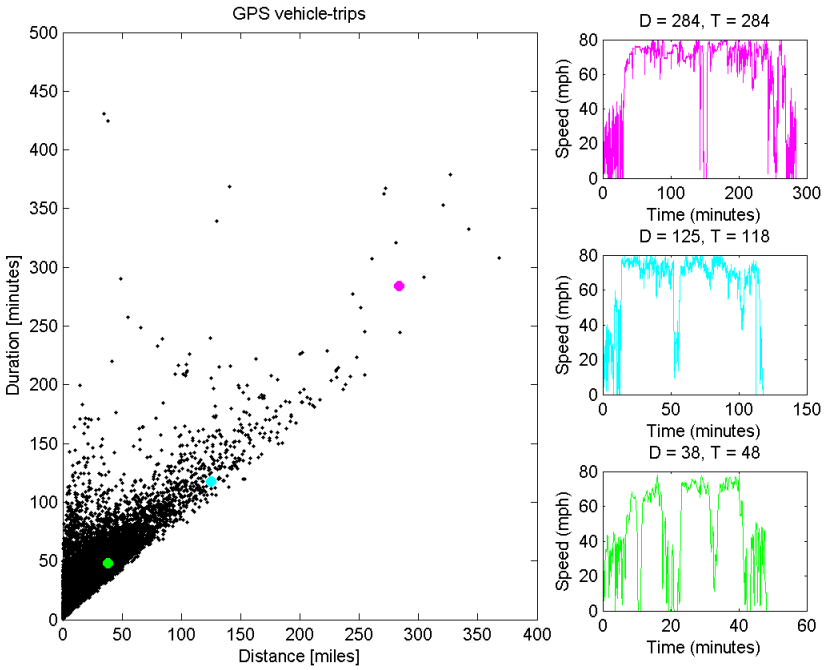

Figure 5-3: Drive cycles of GPS trips with various distances and durations. The displayed drive cycles are shown in a scatterplot of duration versus distance.

5.2 Energy requirements of vehicle travel

This section presents the results of the energy model. These are the results that use the model developed in Chapter 4.

5.2.1 Travel energy requirements

This section introduces the main results of the model, which are the energy requirements of travel. The model output of interest is the amount of usable energy that a battery must provide in order for an electric vehicle to traverse a trip of a given distance and duration. This is called the travel energy requirement of a vehicle-trip, or battery energy (as distinct from tractive energy). The distribution of travel energy requirements for GPS vehicle-trips, NHTS vehicle-trips, and NHTS vehicle-days are shown as histograms in Figure 5-4. The NHTS survey weights have been taken into account in generating the weighted histogram shown.

The first observation is that the GPS and NHTS distributions are similar, as expected, because the distributions of distance and duration are similar as well. The next observation is that vehicle-day energies are larger than vehicle-trip energies, as expected, since vehicle-days are aggregations of vehicle-trips. On average, there are about 4 vehicle-trips per vehicle-day.

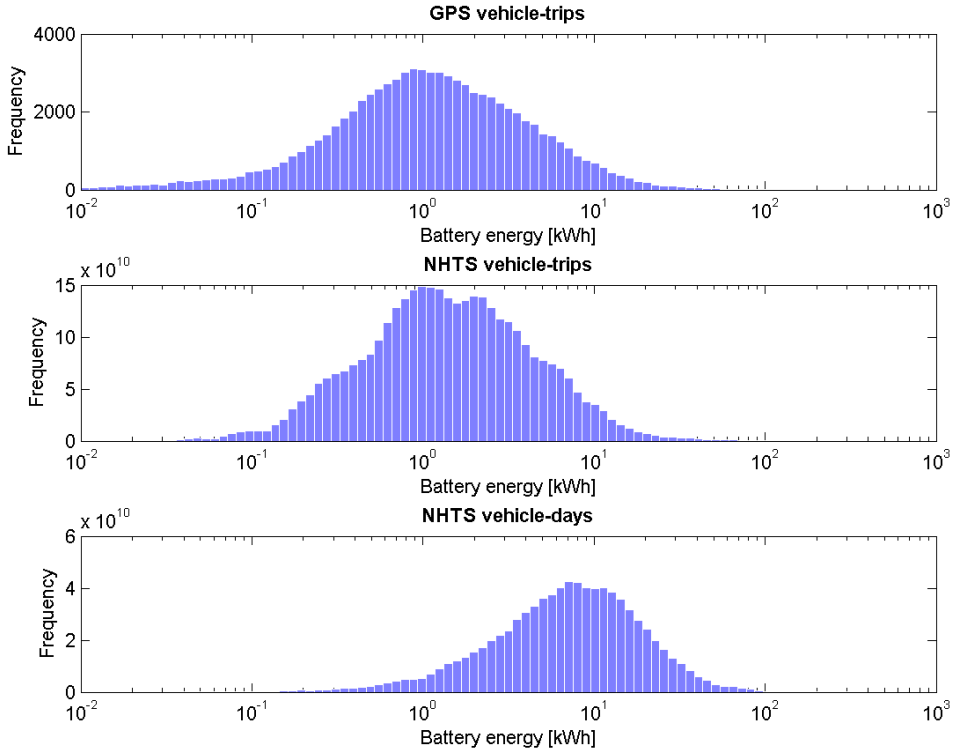

Figure 5-4: Histogram of travel energy requirements for GPS vehicle-trips, NHTS vehicle-trips, and NHTS vehicle-days. The x-axis corresponds to usable battery energy.

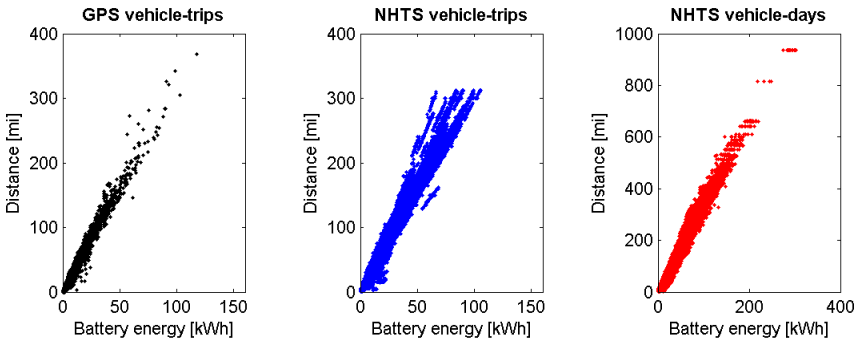

Figure 5-5: Scatterplot of travel energy requirements (E) versus D, for GPS vehicle-trips, NHTS vehicle-trips, and NHTS vehicle-days.

5.2.2 Variability in energy-distance relationship

Next, Figure 5-5 shows a scatterplot of travel energy requirement E versus distance D. In all three units of analysis, E and D are positively correlated, as expected from the derivation of tractive energy in Section 4.1.

This graph to quantifies the variability in the relationship between energy and distance. For example, the energy requirement for vehicle-trips that are 50 miles long range from 11 to 20 kWh for GPS trips, or 10 to 24 kWh for NHTS trips. Understanding this variation will be crucial for calculating accurate estimates of tail fractions, since they are especially sensitive to changes in the distribution of travel energy requirements.

While the relationship between E and D is mostly linear, there is variation around the linear relationship, which is due to differences across drive cycles. Variation in energy consumption due to drive cycles has been identified in previous studies and is expected [78]. While this could be treated as random noise and energy consumption could be predicted from distance by fitting a regression to these results, better results can be achieved with our method. A simple way could be to use a regression to predict E from D. With no intercept term, this is essentially the same as picking a single value for fuel economy, which is not ideal.

The next topic of analysis is the ratio of travel energy requirements to distance, also referred to as travel energy intensity (E/D). Figure 5-6 shows both a histogram of travel energy intensity and a scatterplot of it versus distance. This figure only shows GPS data, because the NHTS data is identical, having been bootstrapped from the GPS data. There is a sharp peak around 0.3 kWh/mi, which agrees well with Kintner-Meyer et al.'s energy intensity of 0.26 kWh/mi for electric compact sedans [51].

There are two features to note in Figure 5-6. First, the average energy intensity increases slightly with increasing trip distance. Properly incorporating the variation in energy intensity with different types of trips is crucial to accurate estimation of travel energy requirements, and this is something our method does naturally through the conditional bootstrap procedure. Secondly, the variance in energy intensity decreases with increased distance. This effect means that the bootstrap procedure can

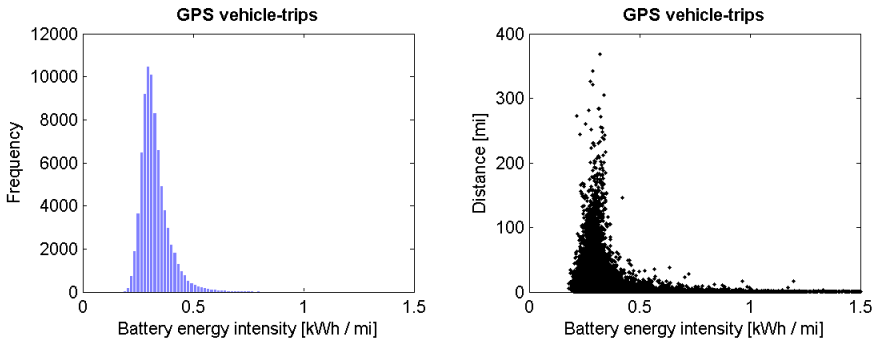

Figure 5-6: Histogram of energy intensity (E/D), and scatterplot of energy intensity versus D.

provide acceptable estimates of required travel energy for long-distance trips, despite sampling from a fewer number of long-distance GPS trips.

5.3 Battery benchmarks and travel energy requirements

This section compares the distribution of travel energy requirements from the previous section to benchmarks for the energy capacity of batteries. Before performing the comparison, a useful metric for comparison is defined, as well as the concept of usable energy in a battery.

5.3.1 Definition of tail fractions of travel energy requirements

The metric that will be used to compare benchmarks of battery energy capacity against the distribution of energy requirements is the "tail fraction", which is defined as the fraction of trips above a given amount of energy. The tail fraction for a given battery energy capacity represents the fraction of trips that would not be possible with the given battery energy capacity. In the context of the model and results, the tail fraction represents the portion of trips with energy requirements that are too high to be met by the 2011 Nissan Leaf. Tail fractions can also be applied to other trip characteristics, such as distance and energy. These tail fractions represent the proportion of distance or energy associated with the trips in the tail fraction, which are not satisfied by the given battery. For clarity, the original definition will be referred to as "travel tail fraction".

Figure 5-7 shows the value of three types of tail fractions at various energy benchmark values, for each unit of analysis. Note that the line plot of the tail fraction is equal to 1 minus the cumulative distribution function (CDF) of the distribution of travel energy requirements, i.e. $TF(E) = 1 - CDF(E)$.

5.3.2 Definition of usable battery energy

The benchmarks for battery energy capacity are in terms of usable energy, rather than nominal battery capacity. For example, the Nissan Leaf battery's nominal

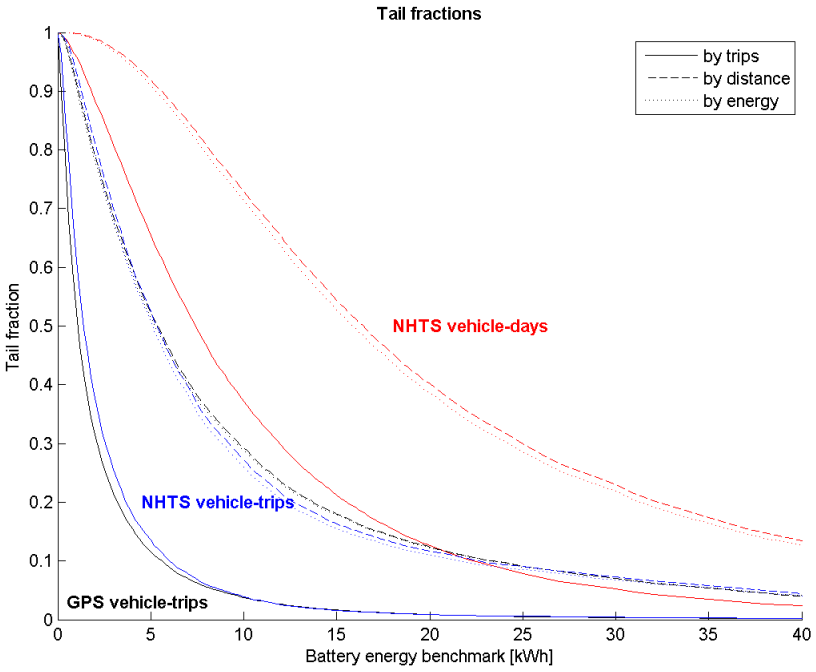

Figure 5-7: Tail fractions of travel, distance, and energy, for GPS vehicle-trips, NHTS vehicle-trips, and NHTS vehicle-days. Tail fractions of distance and energy represent the amount of distance or energy associated with the trips in the travel tail fraction.

capacity is 24 kWh, but its usable energy is estimated be to only 70% of that amount - 16.8 kWh.

The usable amount of energy in a battery is less than the nameplate or nominal energy that is often reported by the automaker or battery maker [79]. The "usable energy" of a battery is defined as the amount of energy that can be extracted at high enough power to be useful for the battery's purpose (i.e. enough power to move the car). Not all energy stored in the battery can be utilized by the vehicle, because at extreme SOC levels, the battery cannot meet the requirements of vehicle operation: at low SOC, batteries have insufficient discharge power; at high SOC, batteries have insufficient regenerative power [5, 59]. This results in a usable SOC window for the battery that is less than 100%. Usable SOC windows vary by vehicles and designs, and can range from 50% for lithium-ion [59] to 70% for PHEVs [75].

The calculated energy requirements for travel should be compared to the usable energy capacity of batteries, not the nameplate value. A usable SOC window of 70% is assumed for the Nissan Leaf, meaning that the energy benchmark that will be compared to is 70% of the Leaf's battery's nominal capacity. The value of 70% was chosen because the same value was used by Pesaran et al. [75][1]. This is a moderate estimate, because a calculation of usable energy based on EPA data, shown in Table 5-1, yields a lower SOC window of 65%, while some anecdotal evidence[2] claim usable SOC windows as high as 87.5%.

It is important to note that the usable SOC window is a different concept from partially charging the battery. Some car makers recommend charging the battery only partially, to avoid negative impacts on battery longevity from to deep recharge-discharge cycles. For example, the Nissan Leaf has a built-in "Long Life" charging mode that charges the battery to only 80% full in order to improve its longevity[3]. However, even if the battery is charged to "100% full", it is impossible to use the full nominal capacity of the battery, for the reasons stated above.

5.3.3 Comparison of battery benchmarks to travel energy requirements

To give context for the distribution of travel energy requirements, it is compared to several benchmarks for energy capacity of vehicle batteries. There are four benchmarks of interest: the current 2011 Nissan Leaf battery, ARPA-E's specific energy target, and USABC's targets for specific energy and total usable energy [90]. The values of these benchmarks, with accompanying tail fractions, are shown in Table 5-2. Figure 5-8 illustrates the comparison between these benchmarks and the distribution of travel energy requirements with a histogram. Figure 5-8 shows that the battery energy capacities specified by the targets fall in the upper tail of the distribution. The tail fractions reported in Table 5-2 give a more precise estimate of the fraction of trips that lie above the targets. While the energy targets are given

[1] Although Pesaran et al. analyzed PHEVs, batteries for both BEVs and PHEVs must provide for all-electric driving, and thus one would expect their designs to be similar enough to assume the same SOC window.

[2] `http://insideevs.com/real-world-test-2013-nissan-leaf-range-vs-2012-nissan-leaf-range/`

[3] `http://www.nissan-techinfo.com/refgh0v/og/leaf/2013-nissan-leaf.pdf`

Table 5-1: Calculation of 2011 Nissan Leaf SOC window using EPA data [101]. The EPA provides the maximum ranges of the Nissan Leaf when driven on both the standard City and Highway cycle [4]. Since the battery was fully drained in these tests, the resulting ranges provide a starting point for estimating the battery's usable energy. First, the unadjusted fuel economy values are converted to electrical energy and a 90% correction for charger efficiency is used to find the battery electricity consumption, in kWh per mile. This is multiplied by the range to find the total energy consumed, then divided by the nominal capacity of 24 kWh to find the usable SOC window. The results are self-consistent, since the SOC window is near 65% for both drive cycles.

Drive cycle	City	Highway
EPA unadjusted fuel economy [MPG-equivalent]	151.5	131.3
EPA range [mi]	77.165	67.316
Battery electricity consumption [kWh/mi]	0.20	0.23
Total energy consumption [kWh]	15.4	15.55
% of 24 kWh nominal capacity	64%	65%

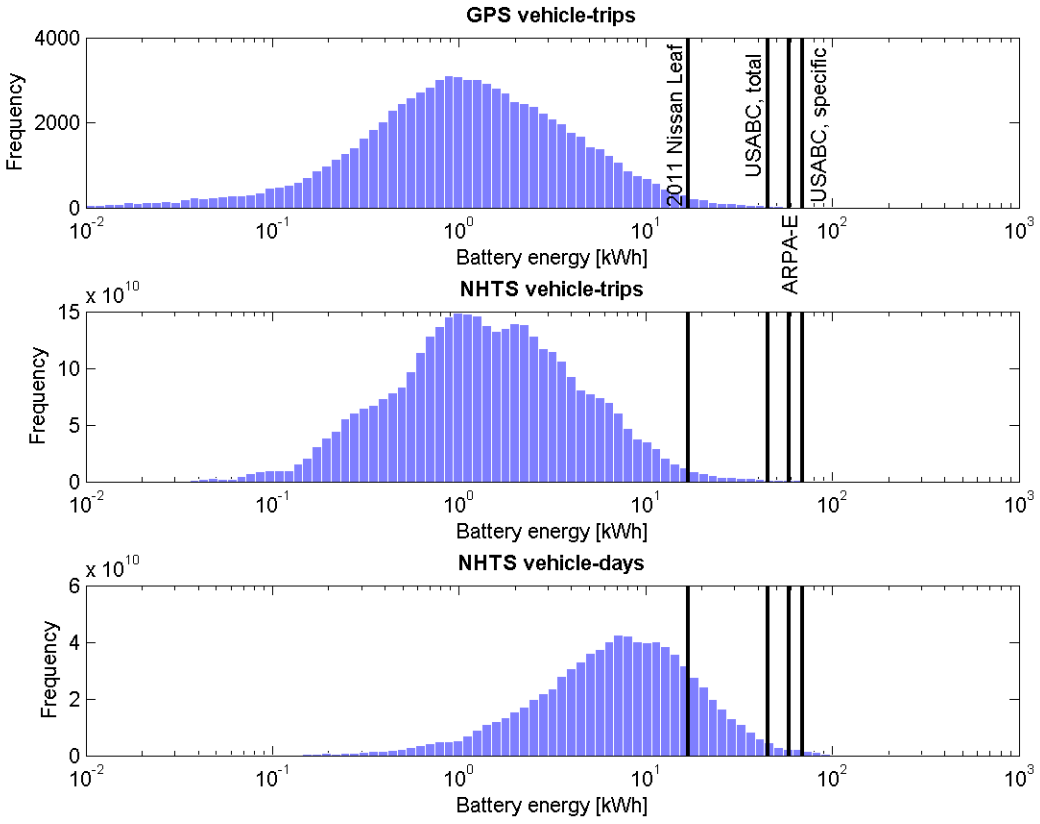

Figure 5-8: Comparison of histogram of travel energy requirements for batteries with benchmarks for battery capacity.

Table 5-2: Benchmarks for battery energy capacity, with corresponding tail fractions. Sources for the energy targets are [90, 7].

Benchmark name		current battery (Nissan Leaf)	USABC target (total E)	ARPA-E target (specific E)	USABC target (specific E)
Energy benchmark [kWh]		16.8	45	58.8	69.09
GPS	Travel tail fraction	1.3%	0.1%	0.1%	0.0%
	Distance tail fraction	15.5%	3.0%	1.6%	0.8%
	Energy tail fraction	15.3%	3.1%	1.6%	0.9%
NHTS trips	Travel	1.3%	0.2%	0.1%	0.0%
	Distance	14.4%	3.4%	1.9%	0.9%
	Energy	13.6%	3.2%	1.7%	0.8%
NHTS days	Travel	17.4%	1.8%	0.9%	0.5%
	Distance	48.6%	10.8%	6.6%	4.1%
	Energy	47.0%	10.1%	6.1%	3.7%

at a specified discharge rate, comparing them with each other and with the Nissan Leaf battery is reasonable because the power requirements for driving stay in a range narrow enough to not significantly affect energy, as explained earlier in Subsection 4.3.3.

Total energy was calculated from the ARPA-E and USABC specific energy targets by multiplying by the 2011 Nissan Leaf's battery pack weight, which is 294 kg. The total energy associated with the USABC specific energy target is different from the USABC total energy target because the USABC's set of targets implicitly assume a smaller battery system mass of 191 kg. Both of these targets are used in the analysis because they represent different contingencies with different battery pack weights.

Table 5-2 indicates that tail fractions of energy are much larger than those for travel only. This is because the longer trips have higher energy requirements, and so carry more weight in the calculation of energy tail fractions. Distance tail fractions are similar to those of energy, because of the similarity between trip distance and trip energy.

Existing batteries can provide for a large portion of vehicle-trips. As shown in Table 5-2, the NHTS vehicle-trip tail fraction of travel for current batteries is 1.3%. The energy associated with these trips accounts for 13.6% of the total energy requirement for all NHTS vehicle-trips combined. Batteries that meet the targets perform even better: the lowest energy target, USABC's total energy target, falls short of the energy requirements for only 0.2% of vehicle-trips, which account for 3.2% of energy.

On the other hand, existing batteries cannot provide for a significant fraction of vehicle-days. The NHTS vehicle-day tail fraction of travel for current batteries is 17.4%. The fraction of total energy associated with these missed trips is much larger - 47.0%. Batteries that meet the target significantly increase the fraction of possible vehicle-days. By meeting the USABC total energy target, the usable battery energy

is increased by three-fold, from 16.8 to 45 kWh, and the vehicle-day tail fraction of travel is reduced to 1.8%. These missed trips account for 10.1% of energy. Meeting the USABC specific energy target, which calls for a four-fold increase in usable energy, would reduce the tail fraction further to 0.5%, which accounts for 3.7% of energy.

As discussed earlier, the individual vehicle-trips that exceed the tail fractions are long highway trips, uncharacteristic of regular commute trips. Vehicle-days above the tail fraction, on the other hand, may consist of a mix of driving on highways and surface roads.

Chapter 6

Discussion

6.1 Contributions to travel energy modeling

This section explains the contribution of this research the study of energy requirements for vehicle travel. Specifically, it describes the ways in which our model can improve on past methods for calculating the battery energy requirement of vehicle trips in cross-sectional travel databases that contain only distance and duration trip information.

6.1.1 Improved accuracy in travel energy estimation

The method presented in this thesis improves upon previous methods for estimating the energy requirement for vehicle travel in three main ways: having a wider scope, accounting for variations in drive cycles, and using real-world drive cycles. This is accomplished by taking advantage of large GPS datasets that have recently become available and large cross-sectional travel surveys.

The first advantage of our approach is that it retains the wider demographic and geographic scope of the NHTS data. So far, GPS datasets have been limited in geographic scope, so previous studies of vehicle energy consumption that use them have been similarly limited [37]. The bootstrap procedure presented here offers a way to incorporate information from GPS data into larger-scale cross-sectional travel studies. With this new method, vehicle energy consumption is analyzed on a broader scale, allowing conclusions to be made about nationwide battery performance targets. In addition, this will enable comparisons of vehicle energy requirements between different geographic regions or market segments, which would be impossible using only GPS data that is confined to smaller sample sizes and specific geographic regions.

The second advantage is that the method accounts for variation in energy intensity with drive cycles, thus improving the accuracy of metrics that depend on the distribution of energy, such as tail fractions. Previous studies have acknowledged that energy intensity varies with drive cycle [37], noting that using a constant value for per-mile energy consumption ignores variations due to traffic, higher acceleration rates, and highway versus city driving. While these variations can be easily accounted for in the GPS datasets that contain drive cycles, our contribution is to offer a method that accounts for these variations when using cross-sectional travel

surveys that cover larger geographical areas but lack detailed drive cycle information. The variation in energy with respect to drive cycles is built into the distributions of energy requirements shown in the results. This improves the accuracy of later analyses, such as the evaluation of performance targets, over using a single value for energy intensity, which would underestimate the spread in the distribution.

Finally, our estimates of energy consumption are closer to reality because they are based on drive cycles obtained from real-world driving, instead being based on standardized or synthetic drive cycles. In the place of real-world drive cycles, previous studies of the impact of variation in drive cycle on vehicle energy consumption have used either standardized cycles from different countries [47] or synthesized naturalistic drive cycles [55]. Previous analyses using only GPS data have been limited by sample size [6]. The approach present in this thesis takes advantage of the real-world drive cycles from large-sample GPS travel surveys that are now available, which are a better representation of reality than the standardized or synthetic drive cycles.

6.1.2 Appropriate application of the travel energy model

The method presented in this thesis estimates travel energy requirements based on a single vehicle and a cross-sectional dataset of vehicle-trips, which makes the results suitable for certain applications but inappropriate for others. The results can be interpreted as the distribution of the Nissan Leaf's vehicle-day energy requirements for all vehicle-days driven in the US in 2009.

Importantly, the results can be used to estimate the fraction of vehicle-days that can be driven by the 2011 Nissan Leaf, but not the fraction of vehicles that can be replaced. The results indicate that the 2011 Nissan Leaf can satisfy the energy requirements of 83% of vehicle-days, but it would satisfy a smaller proportion of the lifetime energy requirements of vehicles. A longitudinal study would be required to address such questions [73]. For example, an existing gasoline vehicle could be replaced by an EV only if the EV can meet nearly all of the vehicle-day energy requirements over the lifetime of the vehicle. The NHTS data is cross-sectional, as opposed to longitudinal, so it lacks the information about the variation in vehicle-days experienced by a single vehicle over its lifetime.

Therefore, these results could apply to vehicle sharing programs, but not to the modeling of vehicle purchases. Vehicle sharing programs are an example where looking at vehicle-days independently of vehicles makes sense, because a traveler can decide to use a shared vehicle if that vehicle can meet the energy requirement for the intended trip, regardless of the other trips the shared vehicle takes over time. On the other hand, evaluating the trip energy requirements for a particular vehicle over time is important when considering what existing vehicles can be replaced by EVs, because it is a factor in vehicle purchase decisions.

Another application of the method is for the analysis of hypothetical scenarios, which can be useful for policy, as will be discussed in Section 6.2. The results represent the hypothetical maximum utilization of a given vehicle, and not the actual energy consumed over the trips recorded in the NHTS. The distribution of energy requirements is calculated using a single electric vehicle, and not the variety of vehicles that were actually used for the recorded trips. In particular, the model estimates the proportion of vehicle-trips that can possibly be achieved by a specific

vehicle and vehicle battery. The results represent the contingency of maximum utilization of the vehicle, in which it is used for all trips it can satisfy. The actual utilization of the vehicle achieved in the real world would be influenced by additional factors such as consumer purchasing decisions and vehicle stock turnover rates.

6.2 Contributions to evaluating technologies and policy

This section discusses the implications of our method on performance targets. There are three quantities that will be compared to each other in this section: performance targets, current technology, and the requirements for travel. Tail fractions, as defined in Section 5.3, are used as the basis for these comparisons, because tail fractions translate battery energy capacity metrics into the physical performance metrics that consumers and policymakers are most concerned with.

The following discussion of performance targets focuses on vehicle-days as the unit of analysis, because they correspond to the energy requirements of full days of driving with overnight charging only, which is how EVs will likely be used, due to the inconvenience of charging between trips. The focus will be on the targets for specific energy and total energy, because these quantities are the most important determining factors of EV performance, notably all-electric range, as explained in the Background in Chapter 2.

6.2.1 Evaluation of existing performance targets

The existing performance targets call for a substantial increase in battery energy capacity, which leads to an increase in the amount of vehicle-days that can be achieved. The ARPA-E and the USABC specific energy targets are 3.5 and 4.1 times the 2011 Nissan Leaf battery's usable specific energy. As shown in Table 5-2, the Leaf's battery cannot provide for 17.4% of vehicle-days, whereas a battery that met the USABC specific energy target would only fail to provide for 0.5% of vehicle-days. Having battery technology that meets the targets would enable EVs to be used for a greater proportion of vehicle-days, which would reduce the use of gasoline vehicles and potentially reduce CO_2 emissions.

The benefit from meeting performance targets is even greater when measured in terms of energy. The 17.4% of vehicle-days that the Nissan Leaf battery cannot provide for accounts for 47% of all energy spent in personal vehicle travel. A battery that meets the USABC specific energy target would reduce the tail fraction of energy for vehicle-days from 47% to 3.7%.

The results show that there is significant room for improvement for current batteries. While the Nissan Leaf can satisfy most vehicle-days (82.6%), they satisfy a smaller proportion of energy (53%). The ability of EVs to offset gasoline usage would be improved with better batteries that provide more range. A battery that meets the USABC specific target could potentially provide for a high proportion of personal vehicle trips and energy (96.3%).

Based on this analysis, the existing performance targets are appropriate. The targets are high enough such that, for batteries that meet the targets, the potential for offsetting petroleum use would not be limited by technology performance but by

adoption rates. For example, an EV with a battery that meets the lowest target, the USABC total energy target, would be able to electrify up to 98% of vehicle-days in the US, which account for 90% of energy consumption. A larger portion of vehicle-days would be possible with access to public charging stations. Therefore, if EV batteries met one of these targets, the main obstacle to offsetting petroleum use with EVs would not be whether EV performance meets the needs of the trips driven, but whether consumers are willing to purchase EVs to replace existing gasoline vehicles.

Even though the existing targets call for an aggressive increase in usable energy capacity (a three- to four-fold increase), the targets are not too high. There are trips whose energy requirement is higher than the target, meaning that the target is not so high that the additional energy capacity would never be used during driving. Rather, all of the additional usable energy that the targets call for contribute to increasing the number of possible trips for the battery. However, since only a small amount of trips require large amounts of energy, a more careful assessment of the appropriateness of targets would need to consider the real-world trade-offs in meeting high targets for energy capacity.

6.2.2 Trade-offs in setting performance targets

In addition to evaluating existing targets, an important question to ask is, "how high should the specific energy target be?" Our model helps to design more effective performance targets because it provides more information to help deal with the inherent trade-offs.

The marginal benefit of additional battery capacity decreases with larger battery capacity. The CDF of the distribution of energy requirements is increasing quickly near the Leaf's energy capacity, but it increases much less quickly near the targets. This is why large improvements in tail fraction can be achieved in moving from the Leaf's energy capacity to the target values, but further increases in energy above the targets will have small effect.

In addition to having reduced marginal performance benefits, high targets for energy capacity also incur opportunity costs, because prioritizing the meeting of a high specific energy target may reduce performance in other goals like cost, longevity, or safety. At some point, the cost of having high energy capacity outweighs the performance returns. Tail fractions calculated with our model provides the information about the marginal performance benefits that is required for such an analysis. Tail fractions of energy can be converted into a quantity of gasoline that is offset, and then into CO_2 emissions prevented, which is a quantity that is easier to use in policy analysis.

6.3 Future work

This section offers ideas for improvements that can be made upon this work. There are several opportunities to improve the accuracy of the travel energy model and to adapt the model for other applications.

6.3.1 Improving accuracy with vehicle simulation software

The accuracy of the model for battery energy requirements could be improved by using simulation software that can accurately model an electric vehicle. Instead of using the empirical formulation of tractive energy and a cycle-averaged powertrain efficiency, battery energy requirements could be directly calculated with the simulation for each GPS drive cycle. The conditional bootstrap procedure would still be used to match the GPS energies with the NHTS trips.

The advantage of using a simulation to calculate energy is that it can provide more accurate calculations because it uses detailed component efficiency maps, which calculate efficiency of vehicle components efficiency depending on the instantaneous operating condition. These detailed component efficiency maps give the efficiency of a particular component (e.g. electric motor) over a range of performance situations, such as rpm or torque. The efficiency maps and other aspects of the simulation provide a more accurate estimation of powertrain efficiency, and intrinsically account for how powertrain efficiency changes with drive cycle.

One difficulty of implementing such a simulation is tuning it to accurately represent reality. For example, energy consumption estimated by the default EV model in the ADVISOR simulation, designed in 2003, doesn't match up well with EPA's measurements: the simulation predicts that more energy is consumed in the City cycle than the Highway cycle, but in reality the opposite is true. The subtleties of real-world operation, such as regenerative braking efficiency or auxiliary power load, must be accounted for to create accurate results.

6.3.2 Accounting for elevation change in tractive energy

While elevation change is neglected in the current model, slight improvements to accuracy could be realized if it were properly accounted for. If GPS drive cycles contained elevation data, a method could be devised to account for this factor. A new term to account for change in potential energy, $mg\Delta z$, would need to be added to the tractive energy formulation.

The typical size of the $mg\Delta z$ term can provide a sense of the the impact of elevation change on tractive energy requirements. Consider a trip from Albuquerque to Santa Fe, which is about 60 miles long and has an elevation gain of about 600 meters. Using the EPA's reported energy intensity for the 2011 Nissan Leaf of $0.34\,\mathrm{kWh/mi}$ and disregarding the elevation change, the energy required for the trip is 20 kWh. The Leaf's mass is 1525 kg, so $mg\Delta z = (1525\,\mathrm{kg})(9.8\,\mathrm{m/s^2})(600\,\mathrm{m}) = 2.5\,\mathrm{kWh}$. Thus, the elevation gain would add about 10% to the tractive energy required. Similar calculations for shorter trips in hilly cities (e.g. San Francisco) show that elevation gain can contribute up to 25% to trip energy requirements.

The expected impact of accounting for elevation change on the distribution of vehicle-trip energy requirements would be to increase the spread of the distribution, because the energy requirement would be increased for uphill trips but decreased for downhill trips. However, the impact on vehicle-day energy requirements is unclear, because most vehicle-days start and end at the same location, and the positive and negative contributions of elevation change would cancel out. Therefore, while the impact on individual trip energy requirements could significant, the size of the impact

on metrics like vehicle-day tail fraction is unclear.

In addition, the effect of elevation on energy use could be larger when comparing different regions, because differing geography could create systematic differences in trip energy requirements between regions. Previous studies have incorporated other factors to improve regional energy estimates, such as accounting for regional variations in weather[1].

6.3.3 Sensitivity to different vehicle parameters

The conclusions in this thesis are based on the analysis of a single vehicle, the 2011 Nissan Leaf. To make a more accurate assessment of the performance level of electric vehicle batteries, the model should account for variations in vehicle design that would affect either tractive energy or powertrain efficiency. For example, heavy vehicles would require more energy capacity for the same performance as lighter vehicles.

The model presented in this thesis would be easy to adapt to other vehicles. The EPA Test Car data files have dynamometer coefficients for all commercially produced vehicles, providing the data required to model tractive energy requirements and powertrain efficiency of other vehicles. A sensitivity analysis could be performed to determine the sensitivity of the tail fractions to changes in vehicle parameters.

6.3.4 Evaluation of performance targets for PHEV batteries

The method proposed here could also be adapted to study PHEVs and performance targets for PHEV batteries. PHEVs are important to study because they, like BEVs, can operate with zero tailpipe emissions, albeit with a shorter all-electric range. In addition, because PHEVs are more appealing to US drivers and are sold in greater numbers, they may have a greater overall climate change mitigation potential.

The all-electric range of PHEVs could be analyzed using the same method used in this thesis. The model would need to be modified to account for the additional complexity of PHEV battery usage, such as accounting for the possibility of charge-sustaining operation and variation in control strategies. Notably, PHEVs would be able to offset portions of long trips whose total energy requirement is greater than that of the battery, by operating in all-electric mode and then switching to gasoline. Because PHEVs have smaller batteries than BEVs, the sensitivity of the tail fraction of trips satisfied in all-electric mode would be greater. Our method would offer similar improvements in accuracy in estimating tail fractions, compared to previous studies [47].

[1] `http://www.eia.gov/consumption/residential/pdf/046405.pdf`

Chapter 7

Conclusion

This thesis addressed the question, "are current targets for energy capacity of EV batteries high enough to meet the demand for travel, based on large datasets on driving habits?" A new method was presented for estimating energy requirements for personal vehicle travel, based on large cross-sectional travel surveys, and it was used to evaluate existing performance targets for battery specific energy. The results indicated that current batteries can satisfy 83% of vehicle-days, which account for 53% of all energy consumed in personal vehicle travel, while batteries that meet the performance targets can satisfy 98 to 99% of vehicle-days, which account for 90 to 96% of energy. Based on these results, existing performance targets for electric vehicle batteries were evaluated and determined to be appropriate. Importantly, these results can be used to quantify the benefits of meeting performance targets, and can help assess technology readiness and guide allocation of research funding. These quantitative results may be updated in a forthcoming paper [61].

Accurate assessment of technologies require detailed understanding of both the technology and the context in which it is used. In the case of electric vehicle batteries, studies that focus on aggregate metrics of transportation, such as sector-wide energy consumption or emissions, often use a constant per-mile vehicle energy consumption. This approach is insufficiently fine-grained provide accurate estimates of EV range, or distributions of energy requirements, because they do not adequately address the variation in energy experienced in real-world driving. This thesis developed an innovative method that combines a detailed vehicle model with a statistical method that combines GPS data with large-scope data. This method is useful for both designing new performance targets and evaluating existing ones.

EVs are important for reducing CO_2 emissions in the personal vehicle sector, so people that create policy to address this subject should be careful to apply the right methods. Estimates of technology performance obtained from appropriate methods will be more accurate, which would improve policymaking through effective allocation of money and effort, and improve the chances of meeting policy goals, such as segmental emissions reduction targets [89]. If performance targets are created using sound methods that accurately represent reality, they can be effective guides for battery research and funding, and ultimately aid in making a more efficient transition to a cleaner transportation sector.

THIS PAGE INTENTIONALLY LEFT BLANK

Bibliography

[1] "Calculation of fuel economy values for labeling," 40 CFR 600.210-08. Available at http://www.law.cornell.edu/cfr/text/40/600.210-08.

[2] "Special procedures related to electric vehicles and plug-in hybrid electric vehicles," 40 CFR 600.116-12. Available at http://www.law.cornell.edu/cfr/text/40/600.116-12.

[3] "Vehicle-specific 5-cycle fuel economy and carbon-related exhaust emission calculations," 40 CFR 600.114-08. Available at http://www.law.cornell.edu/cfr/text/40/600.114-08.

[4] "EPA Test Procedures for Electric Vehicles and Plug-in Hybrids," Available at http://www.smidgeindustriesltd.com/leaf/EPA/EPA_test_procedure_for_EVs-PHEVs-1-13-2011.pdf, 2011.

[5] A123 Systems Inc., "Usable Energy: Key to Determining the True Cost of Advanced Lithium Ion Battery Systems for Electric Vehicles," Available at http://www.a123systems.com/Collateral/Documents/English-US/WhitePapers/UsableEnergywhitepaper.pdf, 2012.

[6] B. Adornato, R. Patil, Z. Filipi, Z. Baraket, and T. Gordon, "Characterizing naturalistic driving patterns for Plug-in Hybrid Electric Vehicle analysis," in *2009 IEEE Vehicle Power and Propulsion Conference*. IEEE, Sep. 2009, pp. 655–660.

[7] Advanced Research Projects Agency-Energy, "Funding Opportunity Announcement - Batteries for Electrical Energy Storage in Transportation (BEEST)," Available at https://arpa-e-foa.energy.gov/Default.aspx?Archive=1, p. p13, 2010, funding Opportunity Number: DE-FOA-0000207.

[8] M. Ahman, "Primary energy efficiency of alternative powertrains in vehicles," *Energy*, vol. 26, no. 11, pp. 973–989, Nov. 2001.

[9] F. An, A. Bando, and M. Ross, "How to drive to save energy and reduce emissions in your daily trip," *Engineering for the Customers: Technical Papers from 25th Fisita Congress Held Beijing 17-21 October 1994*, pp. 75–84, 1994.

[10] F. An and M. Ross, "Model of fuel economy with applications to driving cycles and traffic management," *Transportation Research Record*, 1993.

[11] F. An and D. Santini, "Assessing Tank-to-Wheel Efficiencies of Advanced Technology Vehicles," 2003, SAE Technical Paper 2003-01-0412.

[12] J. Axsen, A. Burke, and K. Kurani, "Batteries for PHEVs: Comparing Goals and the State of Technology," in *Electric and Hybrid Vehicles: Power Sources, Models, Sustainability, Infrastructure and the Market.* Elsevier, 2010.

[13] S. Babaee, A. S. Nagpure, and J. F. DeCarolis, "How much do electric drive vehicles matter to future U.S. emissions?" *Environmental science & technology*, vol. 48, no. 3, pp. 1382–90, Mar. 2014.

[14] I. M. Berry, "The effects of driving style and vehicle performance on the real-world fuel consumption of US light-duty vehicles," Ph.D. dissertation, Massachusetts Institute of Technology, 2010.

[15] A. Boretti, "Analysis of the Regenerative Braking Efficiency of a Latest Electric Vehicle," Nov. 2013, SAE Technical Paper 2013-01-2872.

[16] V. Bosetti and T. Longden, "Light duty vehicle transportation and global climate policy: The importance of electric drive vehicles," *Energy Policy*, vol. 58, pp. 209–219, Jul. 2013.

[17] M. Broussely, "Battery requirements for HEVs, PHEVs, and EVs," *Electric and Hybrid Vehicles*, pp. 305–345, 2010.

[18] E. Burton, J. Gonder, A. Duran, and E. Wood, "Map Matching and Real World Integrated Sensor Data Warehousing," National Renewable Energy Laboratory. Available at http://www.nrel.gov/docs/fy14osti/60893.pdf, 2013.

[19] E. J. Cairns and P. Albertus, "Batteries for electric and hybrid-electric vehicles." *Annual review of chemical and biomolecular engineering*, vol. 1, pp. 299–320, Jan. 2010.

[20] S. Campanari, G. Manzolini, and F. Garcia de la Iglesia, "Energy analysis of electric vehicles using batteries or fuel cells through well-to-wheel driving cycle simulations," *Journal of Power Sources*, vol. 186, no. 2, pp. 464–477, Jan. 2009.

[21] R. B. Carlson, H. Lohse-Busch, J. Diez, and J. Gibbs, "The Measured Impact of Vehicle Mass on Road Load Forces and Energy Consumption for a BEV, HEV, and ICE Vehicle," *SAE International Journal of Alternative Power*, vol. 2, no. 1, pp. 105–114, Apr. 2013.

[22] K. Chau, Y. Wong, and C. Chan, "An overview of energy sources for electric vehicles," *Energy Conversion and Management*, vol. 40, no. 10, pp. 1021–1039, Jul. 1999.

[23] G. Chen and G. L. Yang, "A conditional bootstrap procedure for reconstruction of the incubation period of AIDS," *Mathematical Biosciences*, vol. 117, no. 1-2, pp. 253–269, Sep. 1993.

[24] T. Christen and M. W. Carlen, "Theory of Ragone plots," *Journal of Power Sources*, vol. 91, no. 2, pp. 210–216, Dec. 2000.

[25] J. Cole, "Nissan Europe Releases Spec Sheet on LEAF. Weighs 3,366lbs," http://nissan-leaf.net/2010/10/29/nissan-europe-releases-spec-sheet-on-leaf-weighs-3362lbs/, Oct. 2010.

[26] M. De Gennaro, E. Paffumi, G. Martini, U. Manfredi, H. Scholz, H. Lacher, H. Kuehnelt, and D. Simic, "Experimental Investigation of the Energy Efficiency of an Electric Vehicle in Different Driving Conditions," Apr. 2014, SAE Technical Paper 2014-01-1817.

[27] N. Demirdöven and J. Deutch, "Hybrid cars now, fuel cell cars later." *Science (New York, N.Y.)*, vol. 305, no. 5686, pp. 974–6, Aug. 2004.

[28] J. Drechsler and H. Kiesl, "MI double feature: multiple imputation to address nonresponse and rounding errors in income questions simultaneously," in *Federal Committee on Statistical Methodology*, 2012.

[29] A. Duran and M. Earleywine, "GPS Data Filtration Method for Drive Cycle Analysis Applications," Apr. 2012, SAE Technical Paper 2012-01-0743.

[30] ECOtality, "The EV Project Overview," http://www.theevproject.com/overview.php, 2014.

[31] M. Fellah, G. Singh, A. Rousseau, S. Pagerit, E. Nam, and G. Hoffman, "Impact of real-world drive cycles on phev battery requirements," Apr. 2009, SAE Technical Paper 2009-01-1383.

[32] J. Fu and W. Gao, "Principal component analysis based on drive cycles for hybrid electric vehicle," in *2009 IEEE Vehicle Power and Propulsion Conference*. IEEE, Sep. 2009, pp. 1613–1618.

[33] B. Geller, C. Quinn, and T. H. Bradley, "Analysis of Design Tradeoffs for Plug-in Hybrid Vehicles," in *Electric and Hybrid Vehicles: Power Sources, Models, Sustainability, Infrastructure and the Market*. Elsevier, 2010, p. 159.

[34] C. Giffi, J. Vitale Jr., M. Drew, Y. Kuboshima, and M. Sase, "Unplugged: Electric vehicle realities versus consumer expectations," Deloitte, New York, NY, Tech. Rep., 2011.

[35] T. D. Gillespie, *Fundamentals of Vehicle Dynamics*. Society of Automotive Engineers, Inc., Feb. 1992.

[36] Y. Gogotsi and P. Simon, "Materials science. True performance metrics in electrochemical energy storage." *Science (New York, N.Y.)*, vol. 334, no. 6058, pp. 917–8, Nov. 2011.

[37] J. Gonder, T. Markel, M. Thornton, and A. Simpson, "Using Global Positioning System Travel Data to Assess Real-World Energy Use of Plug-In Hybrid Electric Vehicles," *Transportation Research Record*, vol. 2017, no. -1, pp. 26–32, Dec. 2007.

[38] D. E. Hall and J. C. Moreland, "Fundamentals of Rolling Resistance," *Rubber Chemistry and Technology*, vol. 74, no. 3, pp. 525–539, Jul. 2001.

[39] K. Hartman, "States efforts promote hybrid and electric vehicles," National Conference of State Legislatures. Available at http://www.ncsl.org/research/energy/state-electric-vehicle-incentives-state-chart.aspx, Oct. 2014.

[40] T. R. Hawkins, B. Singh, G. Majeau-Bettez, and A. H. Strø mman, "Comparative Environmental Life Cycle Assessment of Conventional and Electric Vehicles," *Journal of Industrial Ecology*, vol. 17, no. 1, pp. 53–64, Feb. 2013.

[41] H. Helms, M. Pehnt, U. Lambrecht, and A. Liebich, "Electric vehicle and plug-in hybrid energy efficiency and life cycle emissions," in *Proceedings of the 18th International Symposium Transport and Environment, Zurich*, 2010.

[42] C. Hochgraf and M. Duoba, "What if the Prius Wasn't a Hybrid? What if the Corolla Were? An Analysis Based on Vehicle Limited Fuel Consumption and Powertrain and Braking Efficiency," 2010, SAE Technical Paper 2010-01-0834.

[43] X. Hu, N. Murgovski, L. Johannesson, and B. Egardt, "Energy efficiency analysis of a series plug-in hybrid electric bus with different energy management strategies and battery sizes," *Applied Energy*, vol. 111, pp. 1001–1009, Nov. 2013.

[44] I. Husain, *Electric and hybrid vehicles: design fundamentals.* Boca Raton: CRC Press., 2011.

[45] InsideEVs, "Monthly Plug-In Sales Scorecard," http://insideevs.com/monthly-plug-in-sales-scorecard/, 2014.

[46] International Energy Agency, "Key World Energy Statistics," Tech. Rep., Dec. 2013.

[47] O. Karabasoglu and J. Michalek, "Influence of driving patterns on life cycle cost and emissions of hybrid and plug-in electric vehicle powertrains," *Energy Policy*, vol. 60, pp. 445–461, Sep. 2013.

[48] M. J. Kearney, "Electric vehicle charging infrastructure deployment: policy analysis using a dynamic behavioral spatial model," Master's thesis, Massachusetts Institute of Technology, 2011.

[49] J. C. Kelly, J. S. MacDonald, and G. A. Keoleian, "Time-dependent plug-in hybrid electric vehicle charging based on national driving patterns and demographics," *Applied Energy*, vol. 94, pp. 395–405, Jun. 2012.

[50] M. Khan and K. M. Kockelman, "Predicting the market potential of plug-in electric vehicles using multiday GPS data," *Energy Policy*, vol. 46, pp. 225–233, Jul. 2012.

[51] M. Kintner-Meyer, K. Schneider, and R. Pratt, "Impacts assessment of plug-in hybrid vehicles on electric utilities and regional US power grids, Part 1: Technical analysis," *Pacific Northwest National Laboratory*, 2007.

[52] M. Klippenstein, "Electric-Car Market Share In 2013: Understanding The Numbers Better," http://www.greencarreports.com/news/1089555_electric-car-market-share-in-2013-understanding-the-numbers-better, 2014.

[53] M. A. Kromer and J. B. Heywood, "Electric powertrains: opportunities and challenges in the US light-duty vehicle fleet," Master's thesis, Massachusetts Institute of Technology, 2007.

[54] J. Larminie and J. Lowry, *Electric Vehicle Technology Explained*, 2nd ed. West Sussex: John Wiley & Sons, Ltd, 2012.

[55] T. K. Lee and Z. S. Filipi, "Synthesis of real-world driving cycles using stochastic process and statistical methodology," *International Journal of Vehicle Design*, vol. 57, no. 1, p. 17, 2011.

[56] B. Y. Liaw and M. Dubarry, "From driving cycle analysis to understanding battery performance in real-life electric hybrid vehicle operation," *Journal of Power Sources*, vol. 174, no. 1, pp. 76–88, Nov. 2007.

[57] Z. Lin, D. Greene, and M. Gardiner, "FY 2010 Annual Progress Report - Range Optimization for Fuel Cell Vehicles," DOE Hydrogen Program, Tech. Rep., 2009, available at http://www.hydrogen.energy.gov/pdfs/progress10/iii_21_lin.pdf.

[58] N. Lutsey, "A technical analysis of model year 2011 US automobile efficiency," *Transportation Research Part D: Transport and Environment*, vol. 17, no. 5, pp. 361–369, Jul. 2012.

[59] T. Markel and A. Simpson, "Plug-in hybrid electric vehicle energy storage system design," in *Advanced Automotive Battery Conference, May 15-17, 2006 in Baltimore, Maryland.* National Renewable Energy Laboratory, 2006, nREL Report No. CP-540-39614.

[60] T. Markel, K. Smith, and A. Pesaran, "Improving petroleum displacement potential of PHEVs using enhanced charging scenarios," *EVS-24 International Battery, Hybrid and Fuel Cell Electric Vehicle Symposium*, pp. 211–225, 2009.

[61] J. McNerney, M. T. Chang, Z. Needell, and J. E. Trancik, "Energy requirements of personal vehicle travel in U.S. cities," *in final preparation for submission.*

[62] N. Meyer, I. Whittal, M. Christenson, and A. Loiselle-Lapointe, "The impact of driving cycle and climate on electrical consumption and range of fully electric passenger vehicles," *EVS26 - International Battery, Hybrid and Fuel Cell Electric Vehicle Symposium*, Jul. 2012.

[63] C. Mi, M. A. Masrur, and D. W. Gao, *Hybrid Electric Vehicles: Principles and Applications with Practical Perspectives*. John Wiley & Sons, Ltd, 2011.

[64] J. R. Miller, "Applied physics. Valuing reversible energy storage." *Science (New York, N.Y.)*, vol. 335, no. 6074, pp. 1312–3, Mar. 2012.

[65] P. Mock, J. German, A. Bandivadekar, and I. Riemersma, "Discrepancies between type-approval and "real-world" fuel-consumption and CO2 values," The International Council on Clean Transportation, Tech. Rep. 2012-2, 2012.

[66] E. K. Nam and R. Giannelli, "Fuel consumption modeling of conventional and advanced technology vehicles in the physical emission rate estimator (PERE), draft," US Environmental Protection Agency, Tech. Rep. EPA420-P-05-001, 2005.

[67] National Renewable Energy Laboratory, "Transportation Secure Data Center," Accessed January 15, 2014 at www.nrel.gov/tsdc, 2014.

[68] National Research Council, *Effectiveness of the United States Advanced Battery Consortium as a Government-Industry Partnership*. The National Academies Press, 1998.

[69] J. Neubauer, A. Brooker, and E. Wood, "Sensitivity of battery electric vehicle economics to drive patterns, vehicle range, and charge strategies," *Journal of Power Sources*, vol. 209, pp. 269–277, Jul. 2012.

[70] Nissan Motor Corporation, "2011 LEAF - First Responder's Guide," Available at http://www.nissan-techinfo.com/refgh0v/og/FRG/2011-Nissan-LEAF-FRG.pdf.

[71] Nissan Motor Corporation, "LEAF - Technical data," Available at http://newsroom.nissan-europe.com/EU/en-gb/Media/RelatedDocuments.aspx?mediaid=41193, Oct. 2010.

[72] T. Ott, F. Zurbriggen, C. Onder, and L. Guzzella, "Cycle-averaged efficiency of hybrid electric vehicles," *Proceedings of the Institution of Mechanical Engineers, Part D: Journal of Automobile Engineering*, vol. 227, no. 1, pp. 78–86, May 2012.

[73] N. S. Pearre, W. Kempton, R. L. Guensler, and V. V. Elango, "Electric vehicles: How much range is required for a day's driving?" *Transportation Research Part C: Emerging Technologies*, vol. 19, no. 6, pp. 1171–1184, Dec. 2011.

[74] W. Pell and B. Conway, "Quantitative modeling of factors determining Ragone plots for batteries and electrochemical capacitors," *Journal of Power Sources*, vol. 63, no. 2, pp. 255–266, Dec. 1996.

[75] A. Pesaran, T. Markel, H. Tataria, and D. Howell, "Battery Requirements for Plug-in Hybrid Electric Vehicles–Analysis and Rationale," in *23rd International Electric Vehicle Symposium*. National Renewable Energy Laboratory, 2009.

[76] V. A. Petrushov, "Improvement in vehicle aerodynamic drag and rolling resistance determination from coast-down tests," *Proceedings of the Institution of Mechanical Engineers, Part D: Journal of Automobile Engineering*, vol. 212, no. 5, pp. 369–380, May 1998.

[77] D. A. J. Rand, R. Woods, and R. Dell, *Batteries for electric vehicles*. Warrendale, PA. : Society of Automotive Engineers, 1998.

[78] L. Raykin, M. J. Roorda, and H. L. MacLean, "Impacts of driving patterns on tank-to-wheel energy use of plug-in hybrid electric vehicles," *Transportation Research Part D: Transport and Environment*, vol. 17, no. 3, pp. 243–250, May 2012.

[79] P. Reed, "Electric Car Battery Basics: Capacity, Charging and Range," http://www.edmunds.com/car-technology/electric-car-battery-basics-capacity-charging-and-range.html, 2011.

[80] A. Robinson, P. Blythe, M. Bell, Y. Hübner, and G. Hill, "Analysis of electric vehicle driver recharging demand profiles and subsequent impacts on the carbon content of electric vehicle trips," *Energy Policy*, vol. 61, pp. 337–348, Oct. 2013.

[81] San Francisco Bay LEAFs, "Nissan LEAF Info," http://sfbayleafs.org/ev-resources/leaf-info/.

[82] D. J. Santini, A. D. Vyas, D. Saucedo, and B. Jungers, "Where Are the Market Niches for Electric Drive Passenger Cars?" in *Transportation Research Board 90th Annual Meeting*, 2011.

[83] A. Santos, N. McGuckin, H. Nakamoto, D. Gray, and S. Liss, "Summary of Travel Trends: 2009 National Household Travel Survey," US Federal Highway Administration, Tech. Rep., 2011, report No. FHWA-PL-ll-022. Available at http://trid.trb.org/view.aspx?id=1107370.

[84] C.-S. N. Shiau, N. Kaushal, C. T. Hendrickson, S. B. Peterson, J. F. Whitacre, and J. J. Michalek, "Optimal Plug-In Hybrid Electric Vehicle Design and Allocation for Minimum Life Cycle Cost, Petroleum Consumption, and Greenhouse Gas Emissions," *Journal of Mechanical Design*, vol. 132, no. 9, p. 091013, 2010.

[85] V. Srinivasan, "Batteries for Vehicular Applications," Lawrence Berkeley National Laboratory. Available at http://rael.berkeley.edu/sites/default/files/old-site-files/apsenergy/3.4VenkatSMar7.2008.pdf, Mar. 2008.

[86] V. Srinivasan, "The Three Laws of Batteries (and a Bonus Zeroth Law)," Available at https://gigaom.com/2011/03/18/the-three-laws-of-batteries-and-a-bonus-zeroth-law/, 2011.

[87] A. K. Srivastava, B. Annabathina, and S. Kamalasadan, "The Challenges and Policy Options for Integrating Plug-in Hybrid Electric Vehicle into the Electric Grid," *The Electricity Journal*, vol. 23, no. 3, pp. 83–91, Apr. 2010.

[88] M. M. Thackeray, C. Wolverton, and E. D. Isaacs, "Electrical energy storage for transportation–approaching the limits of, and going beyond, lithium-ion batteries," *Energy & Environmental Science*, vol. 5, no. 7, p. 7854, 2012.

[89] J. E. Trancik, M. T. Chang, C. Karapataki, and L. C. Stokes, "Effectiveness of a segmental approach to climate policy." *Environmental science & technology*, vol. 48, no. 1, pp. 27–35, Jan. 2014.

[90] US Advanced Battery Consortium, "USABC Goals for Advanced Batteries for EVs - CY 2020 Commercialization," Available at http://www.uscar.org/guest/article_view.php?articles_id=85, 2013.

[91] US Council for Automotive Research, "USCAR: Energy Storage System Goals," Available at http://www.uscar.org/guest/article_view.php?articles_id=85.

[92] US Department of Energy, "EV Everywhere Grand Challenge Road to Success," Available at http://energy.gov/eere/vehicles/downloads/ev-everywhere-grand-challenge-road-success, 2014.

[93] US DRIVE Partnership, "Electrochemical Energy Storage Technical Team Roadmap," Available at http://www1.eere.energy.gov/vehiclesandfuels/pdfs/program/eestt_roadmap_june2013.pdf, 2013.

[94] US Energy Information Administration, "Methodologies for Estimating Fuel Consumption Using the 2009 National Household Travel Survey," Available at http://nhts.ornl.gov/2009/pub/EIA.pdf, 2011.

[95] US Energy Information Administration, "Annual Energy Outlook 2014," U.S. Energy Information Administration (EIA), Tech. Rep., 2014.

[96] US Energy Information Administration, "Monthly Energy Review August 2014," Tech. Rep., 2014.

[97] US Environmental Protection Agency, "Data & Testing | Fuel Economy," Available at http://www.epa.gov/fueleconomy/data.htm.

[98] US Environmental Protection Agency, "How Vehicles Are Tested," http://www.fueleconomy.gov/feg/how_tested.shtml.

[99] US Environmental Protection Agency, "Test Car List Data Files," Available at http://www.epa.gov/otaq/tcldata.htm.

[100] US Environmental Protection Agency, "Fuel Economy Labeling of Motor Vehicle Revisions to Improve Calculation of Fuel Economy Estimates," Available at http://www.epa.gov/carlabel/documents/420r06017.pdf, Dec. 2006, report No. EPA420-R-06-017.

[101] US Environmental Protection Agency, "Download Fuel Economy Data," Available at http://www.fueleconomy.gov/feg/download.shtml, 2014.

[102] US Environmental Protection Agency and National Highway Traffic Safety Administration, "Final Rulemaking to Establish Light-Duty Vehicle Greenhouse Gas Emission Standards and Corporate Average Fuel Economy Standards - Regulatory Impact Analysis," Available at http://www.epa.gov/oms/climate/regulations/420r10009.pdf, pp. 5–56, Apr. 2010, report No. EPA-420-R-10-009.

[103] US Environmental Protection Agency Climate Change Division, "Inventory of U.S. Greenhouse Gas Emissions and Sinks: 1990-2012," http://www.epa.gov/climatechange/ghgemissions/sources/transportation.html, 2014.

[104] US Federal Highway Administration, "National Household Travel Survey 2009," Available at http://nhts.ornl.gov/.

[105] US General Services Administration, "Electric Vehicle Pilot Program," http://www.gsa.gov/portal/content/281581, 2011.

[106] US Internal Revenue Service, "Plug-In Electric Drive Vehicle Credit (IRC 30D)," Available at http://www.irs.gov/Businesses/Plug-In-Electric-Vehicle-Credit-(IRC-30-and-IRC-30D), Feb. 2014.

[107] R. Van Noorden, "The rechargeable revolution: A better battery." *Nature*, vol. 507, no. 7490, pp. 26–8, Mar. 2014.

[108] A. D. Vyas, D. J. Santini, and L. R. Johnson, "Potential of Plug-In Hybrid Electric Vehicles to Reduce Petroleum Use," *Transportation Research Record: Journal of the Transportation Research Board*, vol. 2139, no. -1, pp. 55–63, Dec. 2009.

[109] C. Weiss, "900hp Quant EV powered by flow cell battery," http://www.gizmag.com/900-hp-supercar-flow-battery/31091/, 2014.

[110] P. Weissler, "Leaf to be sold with battery pack at C-segment price," *Automotive Engineering Magazine*, Mar. 2010.

[111] S. Williamson, A. Emadi, and A. Dewan, "Effects of Varying Driving Schedules on the Drive Train Efficiency and Performance Characteristics of a Parallel Diesel-Hybrid Bus," 2005, SAE Technical Paper 2005-01-3477.

[112] Working Group III to the Fifth Assessment Report of the IPCC, "Transport. In Climate Change 2014: Mitigation of Climate Change." Intergovernmental Panel on Climate Change, Tech. Rep., 2014.

[113] C. Yang, "Fuel electricity and plug-in electric vehicles in a low carbon fuel standard," *Energy Policy*, vol. 56, pp. 51–62, May 2013.

[114] C. Yin and M. Stepp, "Shifting Gears: Transcending Conventional Economic Doctrines to Develop Better Electric Vehicle Batteries," *The Information Technology and Innovation Foundation*, 2012.